GERMAN - MONGOLIAN INSTITUTE FOR RESOURCES AND TECHNOLOGY

The present work was submitted to the Faculty of Engineering

Study on Water hammer in Lime Slurry Pipeline

Bachelor Thesis

by

Turtsetseg Nanjid

Supervisor 1 / Examiner 1	**Ph.D. Odbileg Norovrenchin**
Supervisor 2 / Examiner 2	**Professor Ariunbolor Purvee**

Ulaanbaatar/Nalaikh, 7 May 2019

Statutory Declaration

Nanjid, Turtsetseg	14405689204862
Last Name, First Name	Student ID Number

I hereby affirm in lieu of an oath that I provided the submitted bachelor thesis

xxx

independently and without undue external help. I did not use any sources other than those stated. In case that the work is additionally submitted on a data medium, I declare that the written and the electronic form are completely identical. The work was not submitted in the same or similar form to any examination authority.

Ulaanbaatar, Mongolia, May 24, 2019	
Place, Date	Signature

Acknowledgement

This work has been successfully completed with the help of many people and their guidance and I am privileged to have this throughout the completion of my work. All I have done is due to such supervision and assistance. I also would like to express gratitude towards German-Mongolian Institute for Resources and Technology and Oyu Tolgoi LLC for giving me this great opportunity to work on this project and providing me with the necessary equipment.

I respect and thank Ph.D. Odbileg N. and Prof. Ariunbolor P. for sharing their ideas and supporting me regardless of their busy schedule. Also I highly appreciate MSc Soronzonbold Otgonbaatar for his valuable contribution to helping me figure out the theory and software. Their help is highly valued and should be acknowledged.

I also would like to thank my team members Ulziikhuu O., Tumendelger B., Zolboo B. on the project from Oyu Tolgoi LLC for sharing their findings and perspectives with me, it was very valuable and enrichened my work.

From the company side, special thanks to superintendent Mr. Gurragchaa T., and graduate engineer Mr. Galdan Ts. gave me assistance, guidance and provided me with necessary information.

Finally, I owe my deepest gratitude to my family and friends, it would have been impossible to carry out this project without their support.

Abstract

The present study is intended to examine the effect of water hammer in milk of lime distribution system at Oyu Tolgoi LLC. The company produces copper concentrate and the flotation process for the copper concentrate production requires slaked lime in order to control pH value. It is essential to prevent system failures because of safety and economic purpose.

Specialized engineering software called “Wanda Engineering 4.5” is used to obtain the realization of the effect of water hammer. It concentrates mostly on reducing the water hammer effect because of the damage it is known to be causing. Wanda Engineering 4.5 is powerful software which can theoretically analyze the transient flow of fluid. Transient flow is originated from the sudden change in velocity of the flowing fluid such as pump trip, valve closure, etc. In this study, only valve closure originated water hammer is studied.

Several factors are known to be affecting water hammer effect and for this study, the type of the valve, the valve closure time duration, and profile, a solid concentration of the lime slurry are the major concerns. The finding of the study shows the sensitivity of the water hammer effect from these factors and the optimum value or pattern for some factors.

It was found that the best method to reduce water hammer is stepwise closure of the valve especially rapid closure at the beginning with gradual closure in the end. In overall closure time of 1 second, the uniform closing causes maximum pressure of ~2.9barg and stepwise closure can reduce it to ~2.2barg at the point right before the valve.

The least pressure inducing valve was the butterfly valve to compare to pinch valve, gate valve, and ball valve. The maximum pressure in 5 seconds of butterfly valve closure was 2.053barg and the steady-state pressure was at the same point was 2.023barg.

Table of Contents

List of Figures

List of Tables

1. General Introduction

1.1. Profile of the organization

Oyu Tolgoi LLC was initially found in October 2009 based on the investment agreement between The Government of Mongolia, Ivanhoe Mines Mongolia INC LLC, Ivanhoe Mine LTD, and Rio Tinto International Holdings Limited. However, the trace of the deposit goes back to the late Bronze age and the discovery using modern tools was made in the 1980s by Mongolian & Russian Geochemical Survey Team. According to the investment agreement, the Government of Mongolia owns 34% of the share and the rest 66% is owned by Canadian-based Turquoise Hill Resources. Rio Tinto has a 50.8% interest in Turquoise Hill, therefore it manages Oyu Tolgoi on behalf of the partnership.

The project accommodates three main deposits, which consist of a series of ore bodies containing molybdenum, silver, gold, and copper over 12.4 km stretched land in depth of over 2 km. Southern Oyu deposit is copper rich sulfide mineralization containing in an average 0.81 gram of gold and 1.17 percent of copper in per ton of ore body. It is 1.5 km wide and 2.7 km long and currently being mined using Open Pit mining technique. Hugo Dummet deposit contains 638 meters of rich copper-gold mineralization, lying 222 meters under, then stretching further. It is considered to be one of the world's biggest and high-grade gold-copper porphyry systems. Heruga deposit has a copper-gold rich core and an upper zone of molybdenum-rich ore. The deepest drilling in this deposit has reached 2736m. Both Heruga and Hugo Dummett deposits are planned to be mined using Underground Block-Cave mining method, which is one of the most modern and advanced underground mining technique. At the moment underground mine is under construction and planned to start operating in 2020.

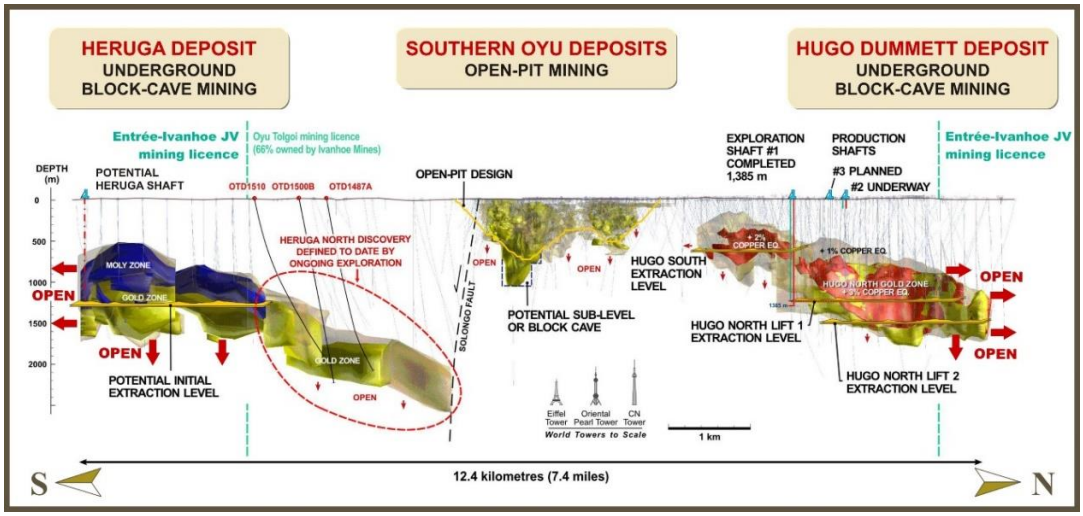

Figure 1.1. Realization of Oyu Tolgoi deposits

1.2. The system at Oyu Tolgoi LLC

In general, there are two common types of hydrated lime feeding system; paste type and detergent type. Paste type hydrated lime feeding system uses high concentrated hydrated lime known as lime paste and this type of system is used at Oyu Tolgoi LLC. On the other hand, there is detention type of system with low concentrated hydrated lime and continuously flowing, which is used at Erdenet Mining Corporation (EMC).

Feeding system of hydrated lime with a low concentration (detention type) has continuous flow, but higher water consumption. Despite having continuous flow, scale in the pipe wall is present. At EMC, yearly cleaning with weak acid takes place to reduce the scale and as they reported, PVC pipe and metal-based alloy pipe has an identical amount of scale by the end of the year. The advantage of detention type feeding system is that the problem of water hammer is insignificant since frequently operating valves are not necessary for the operation.

Paste type of system is advantageous due to low water consumption (an important factor for Gobi area). Crucial characteristics of hydrated lime with high density is that lower settling rate. Starting from a weight concentration of 20% settling rate of the fluid decreases significantly as shown in Figure 1.2. It results in less scale on the pipe wall; however, continuous flow into the system is not applicable. In order to secure an accurate pH balance in the system, hydrated lime flow is controlled using pinch valves with automated opening and closing whenever necessary. Frequent closing and the opening of pinch valves cause water hammer and rapid wear rate of the pinch valves.

Figure 1.2. Settling rates of the hydrated lime for different concentrations [1]

In the system, the pinch valves are located in the branched pipes from the main flow pipeline. Therefore, the effects of water hammer differ from that of simple straight

pipelines. Also, Victaulic couplings are used in order to damp oscillations from water hammer.

1.3. Problem Statement

Oyu Tolgoi LLC produces copper concentrate; thus, processing plants hold significant importance in the company financial profit. In order to produce copper concentrate, copper ore goes under a series of size reduction, flotation and dewatering processes as shown in *Figure 1.3.*

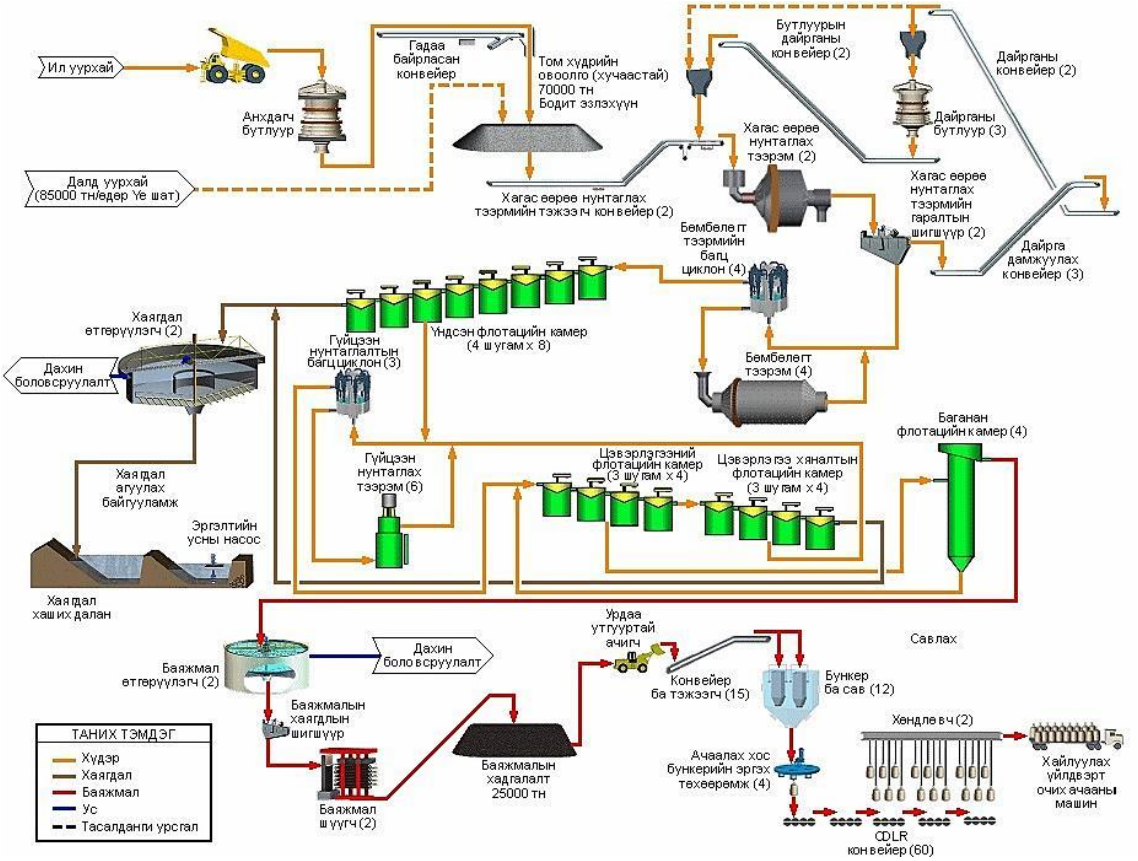

Figure 1.3. Flow diagram of the copper concentrate processing

For the flotation, the balance between reagent dosage and pH plays an important role in selectivity of complex mineral [2]. By balancing pH, higher recovery can be achieved. Lime slaking system is responsible for preparing, storing and distributing lime milk as shown in *Figure 1.3.* Since the pH level should be precisely controlled, any unplanned failure in Lime system can cause a shutdown of the whole process. The distribution system has stand-by pumps and pipes in case of any unplanned failure in the primary distribution. However, the standby system also could fail while the primary system is still under maintenance.

More importantly, major safety issues follow the failure of the pipeline. The flowing fluid in the system is highly corrosive, thus hazardous for a human being as well as the surrounding environment. During the maintenance process, it brings a significant danger of falling object from height as well as requires personnel to work at height. Also, there has been an accident of fallen pipeline in 2013 and as a response, some of the Victaulic couplings are secured from falling as shown in Figure 1.6.

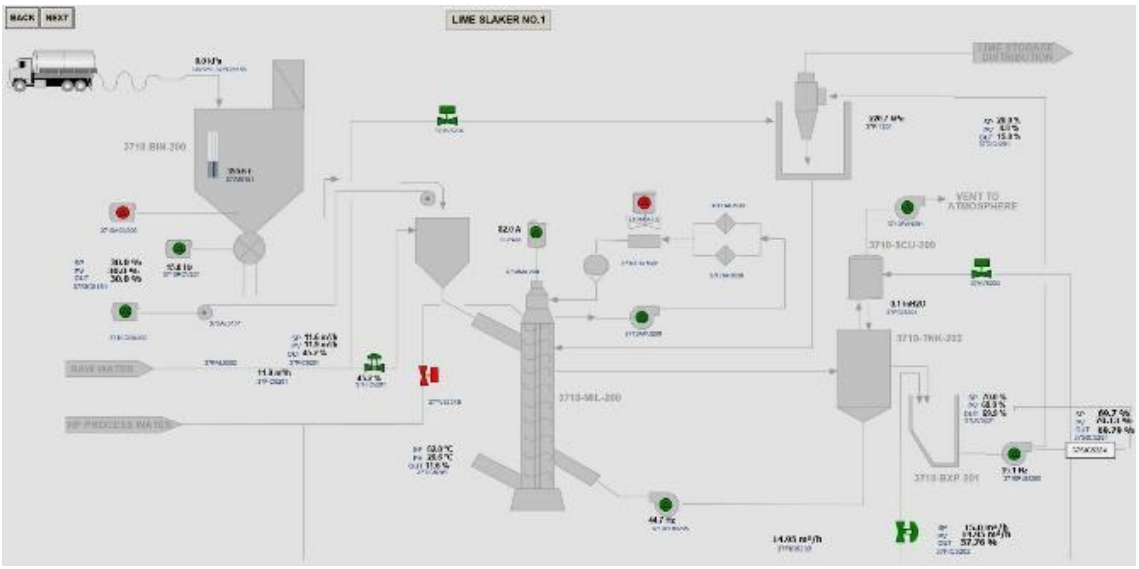

Figure 1.4. Lime Slaker 1 & 2

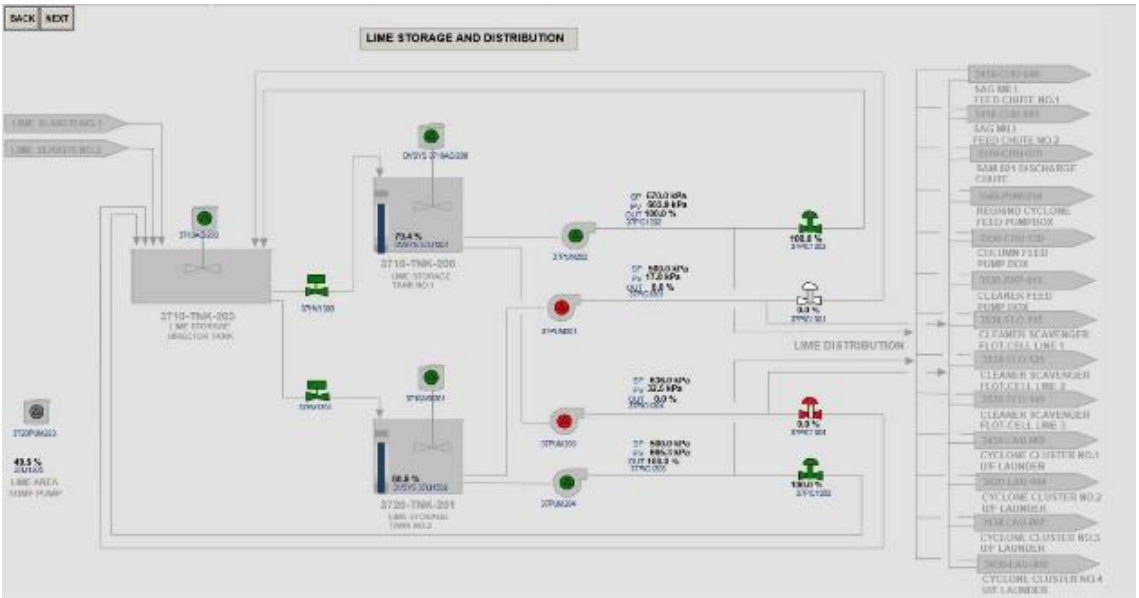

Figure 1.5. Lime Storage and Distribution

Figure 1.6. Current prevention of lime coupling failure. Welded brackets and safety truss.

There are the following problems in the system, which are considered to be threatening:

1. Shift of the distributing pipes

Supply of the lime milk into the grinding and flotation loop is modified by pinch valves and pinch valves periodically open and close with fully automated control. At the moment of closing the valve, the water hammer takes place. The shock wave travels through the pipe causing structural damage and shift of the pipes as shown in Figure 1.2.5. It holds danger of falling object from height and capability of causing fatal injuries.

2. Scaling in the distributing pipes

During distribution, pipes get blocked due to accumulation especially in elbow fittings and vertical pipes. Increased pressure can be caused and affect the system.

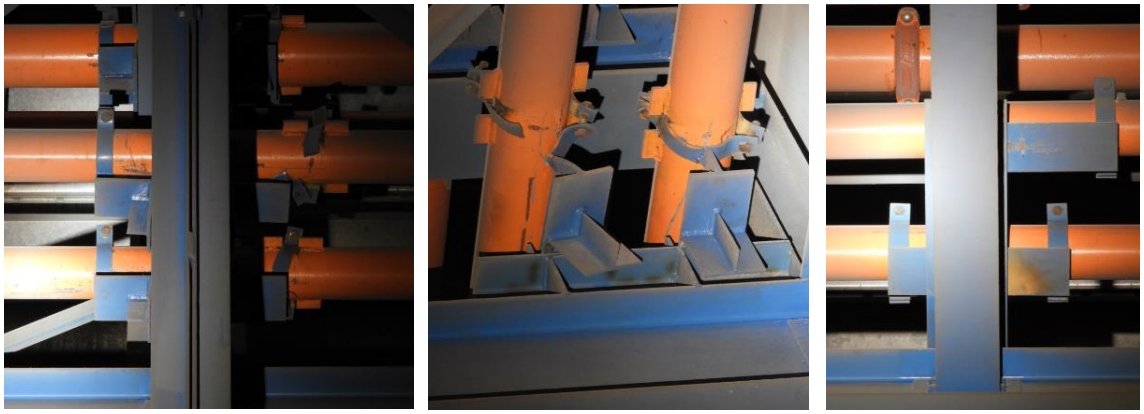

Figure 1.7. Structural damage and shift of the pipes

3. Overflow in the lime tank

Due to overloading of the distribution lines and pumps, most of the hydrated lime cycle back to the tank and cause overflow.

4. High temperature on the bearings of distribution pumps

Bearings work under high load because of overloaded distribution pumps. This leads to high temperatures on the bearings.

In this study, the phenomenon of water hammer and problems related to the water hammer effect are studied using a simulation software.

1.4. Objective of the study

The objectives of the study are to:

- Develop a system equivalent to the part being considered
- Observe the relationship between valve closure rate and hydraulic transient pressure
- Determine the effect of water hammer reducing methods as well as protection devices
- Find the optimal solid concentration of slurry with respect to the water effect
- Optimize valve closure time and profile

2. Literature Review

2.1. The phenomenon of water hammer

In every fluid transportation system in the pipe, valves regulate the flow within the system; which mostly results in a change of discharge. The pressure of the flowing fluid in the conduit and its discharge are bilateral, therefore a change in discharge (e.g. partial or full closure of the valve) induces a corresponding change in pressure and vise versa. The change in pressure caused by this correlation is known as water hammer.

When flowing liquid in conduit suddenly stops, the liquid tries to continue flow in the same direction due to initial inertia. In the area where velocity change develops, the liquid pressure in the pipe shoots up. As it rebounds, the pressure in the nearby region increases forming an acoustic pressure wave which then travels with the speed of sound in that particular liquid. An example of the transient pressure wave at a fixed point in the system is shown in Figure 2.1.

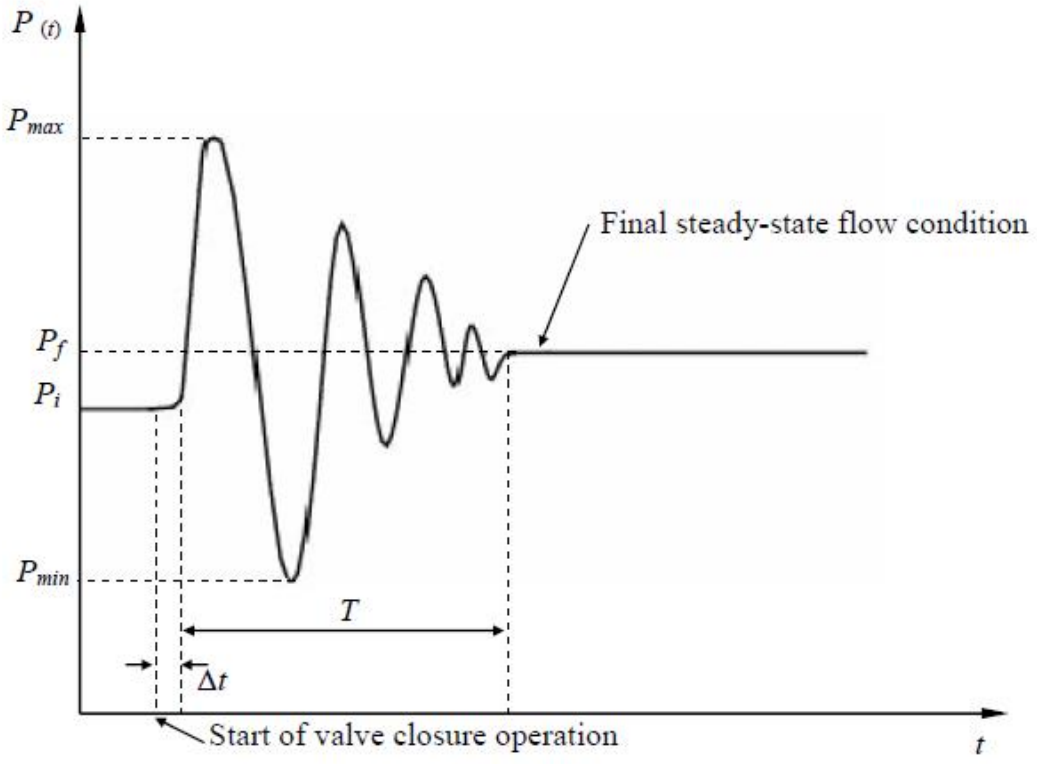

Figure 2.1. Pressure profile of water hammer at a fixed position in the system.

2.2. Impacts of water hammer

A transient wave, as in Figure 2.1., leads to system piping and other facilities to oscillating high and low pressure, and cyclic load and these pressures have fatal effects on the system as a whole.

If the maximum pressures are excessively high, it can lead hydraulic equipment in a pipe network to fail. In case of higher pressures, pipe failure or joint rupture, or bend or elbow movement may occur. On the other hand, low pressures (negative pressures) can result in twist, implosion, and leakage at pipe joints during sub-atmospheric phases. Low-pressure transients are normally experienced on the downstream side of a closing valve.

Sub-atmospheric (low) pressures increase the risk of collapse depending on the pipe material and its geometry. Supposing the pipes do not collapse; however, when the pressure in pipeline drops to vapor pressure of the liquid, it creates column separation (cavitation). The knocking sound of water hammer is caused by

Rapid fluctuations in pipelines are very rapid, as in case of water hammer, which cause cyclic loads. Pipes can burst due to fatigue from a large number of cyclic loads and pipeline fittings, bends and elbows can rupture or leak bringing major safety issues.

2.4. Major factors influencing on water hammer

Many factors influence on the magnitude of the hydraulic pressure peak, it includes:

- The geometry of the pipeline, longer the pipeline is stronger the hydraulic pressure. Multi-branched pipeline systems are more resistant to water hammer (e.g. system at Oyu Tolgoi LLC)
- Pipeline profile
- Valve closure rate. Rapid closure results in higher pressure peak and gradual closure causes less harmful effects.
- The elasticity of the liquid and pipe material. Compressible fluids and highly elastic pipe materials can prevent damage from water hammer.
- Amount of dissolved gas or gaseous gas in the fluid. Typically, gas bubbles damp the oscillations.
- Couplings in the pipeline system, for example, Victaulic couplings reduce the scope of the water hammer by damping the oscillations.
- Protective measures such as surge chambers, air vessels, frequency controlled pumps, etc.

2.3. The theoretical background of water hammer

Researches on water hammer phenomenon date back to the nineteenth century. Fundamental equations lead to two most common formulas:

Joukowsky equation (1898) describes the correlation between maximum pressure change Δp and velocity change Δv [3]

$$\Delta p = \Delta v \cdot \rho \cdot a \tag{1}$$

where ρ = the density of the fluid, kg/m^3

a = wave propagation celerity, m/s

Another equation is *Korteweg equation (1878)* for the celerity of the wave propagation [4]

$$a = \frac{\sqrt{\frac{K}{\rho}}}{\sqrt{1 + \frac{D}{e} \cdot \frac{K}{E} \cdot C}} \tag{2}$$

where K = bulk modulus of the liquid

E = modulus of elasticity of pipe material, Pa

D = pipe diameter, m

e = wall thickness (pipe thickness), m

C = coefficient dependent on the axial and lateral strain of the material, nu

C takes on values:

a) $C = 1$
b) $C = 1 - \frac{\mu}{2}$
c) $C = 1 - \mu^2$

where μ = Poisson's ratio of pipe material, nu

In practice, C can approximated as 1.

Above mentioned two formulas are simplified and approximated for easier calculation as well as mathematical modeling. They are valid at control volume in a pipeline neglecting wave reflection under the assumptions of frictionless flow, elastic pipe as well as compressible fluid. Regardless of their simplicity, they are proven to be useful in practice for describing the phenomenon. Equations (1) and (2) allow us to estimate the maximum

increase in pressure (or decrease in the event of negative water hammer), pressure wave velocity and, therefore, period of pressure oscillations during transient processes in the elastic trumpet. For many years, it was considered satisfactory.

More complex and fundamental equations describing transient flow was developed in form of partial differential equations [3] as follows:

the continuity equation:

$$g \cdot A \cdot \frac{\partial H}{\partial t} + a^2 \cdot \frac{\partial Q}{\partial x} = 0 \tag{3}$$

and the momentum equation:

$$g \cdot A \cdot \frac{\partial H}{\partial x} + \frac{\partial Q}{\partial t} + f \cdot \frac{|Q|Q}{2DA} = 0 \tag{4}$$

where x = space coordinate, m

t = time, s

H = piezometric head, m

g = acceleration due to gravity, m/s^2

f = friction factor, nu

A = cross sectional area of the pipe, m^2

This model in Eqs. (3) and (4) can be applied to flow of compressible fluid in the elastic pipe. These equations are hyperbolic type partial differential equations and can be transformed into two ordinary differential equations (ODE). The following equations are basic algebraic relations describing the transient propagation of pressure head and flow in a pipeline.

$$C^+ : H_i^{n+1} = \frac{C_p}{C_a} + \frac{1}{C_a} \cdot (Q_u)_i^{n+1} \tag{5}$$

$$C^- : H_i^{n+1} = \frac{C_n}{C_a} - \frac{1}{C_a} \cdot (Q)_i^{n+1} \tag{6}$$

where C_p, C_n = constants known for each time step

C_a, R = variable depending on conduit properties

Q_u = upstream discharges

Q = downstream discharges. $C_p, C_n,\ C_a$ and R are formulated in the below mentioned equations [5].

$$C_p = (Q)_{i-1}^n + C_a \cdot H_{i-1}^n - R \cdot \Delta t \cdot (Q_u)_{i-1}^n \cdot |(Q_u)_{i-1}^n| \tag{7}$$

$$C_n = (Q)_{i+1}^n - C_a \cdot H_{i+1}^n - R \cdot \Delta t \cdot (Q_u)_{i+1}^n \cdot |(Q_u)_{i+1}^n| \tag{8}$$

$$C_a = \frac{g \cdot A}{a} \tag{9}$$

$$R = \frac{f}{2 \cdot D \cdot A} \tag{10}$$

2.4. Boundary Conditions for the differential equations

At the downstream, the orifice principle is used to evaluate the valves until the fully closed state and the finite difference equation for positive characteristics is estimated accordingly. The Eqs. 11 applies for steady-state flow through an orifice, which is fully open and will be closed at a specific time [6].

$$Q_i^n = (C_d \cdot A_V)_0 \cdot \sqrt{2 \cdot g \cdot H_i^n} \tag{11}$$

where 0,n = indicators for steady-state conditions

C_d = coefficient of discharge

H_i^n = head upstream of the valve at nth time step

A_V = Area of valve opening

The transient flow equation for $(n+1)^{th}$ time step can be expressed as follows:

$$Q_i^{n+1} = (C_d \cdot A_V) \cdot \sqrt{2 \cdot g \cdot H_i^{n+1}} \tag{12}$$

The relative opening τ is determined as shown below and flow rate for the $(n+1)^{th}$ time steps can be derived as well.

$$\tau = \frac{(C_d \cdot A_V)}{(C_d \cdot A_V)_0} \tag{13}$$

$$Q_i^{n+1} = \frac{Q_i^n}{\sqrt{H_i^n}} \cdot \tau \cdot \sqrt{\Delta H} \tag{14}$$

where ΔH = head loss through the valve.

In the flow condition of the steady-state, flow through the valve is Q_i^n under a head of H_i^n, then $\tau = 1$ and for the simultaneously closed valve, $\tau = 0$ and the pressure heads can be calculated using characteristic line equations Eqs. (5) and (6).

2.5. Water hammer mitigating devices and methods

In order to prevent serious damages from water hammer, many types of control devices are used broadly in industrial applications. Firstly, valve closure rates, pipe sizes, and pumps controls are varied for possibilities to keep the damage at an acceptable level. However, it cannot be freely controlled due to application requirements, therefore, protection devices are designed for satisfying the requirement while preventing damages of water hammer. In Table 1., commonly used water hammer protection devices and their functions are provided.

In order to control minimum pressure in the pipe, the followings can be adjusted or implemented; Pump inertia, Surge tanks, Air chambers, One-way tanks, Air-inlet valves, and Pump bypass valves. For restraining maximum pressure in the line, the following can be implemented; Surge tanks, Relief valves, Air chambers, Pump bypass valves, and Anticipator relief valves. Single device usage or a combination of multi-devices can be implemented [7].

2.5.1. Air chambers and Surge Tanks

The working principle of air chambers and surge tanks is to store or discharge liquid in the event of high-pressure transients and introducing fluid from outside when the pressure is low. Optimally, it should be located near the source of hydraulic transients (valve).

A pressure vessel containing fluid and air volume that is maintained by an air compressor is known as an air chamber. During low-pressure water hammer transient, air chamber expands, forcing fluid from air chamber into the system.

A surge tank is an open standpipe or storage reservoir connected to the hydraulic system. The level of a surge tank is equivalent to the piezometric head of the hydraulic system at that point. When the pressure drops, the elevation of the fluid decreases therefore, stabilizing the hydraulic system.

2.5.2. Pressure relief and other regulating valves

Pressure relief valve protects the system from over pressurization by opening when the pressure exceeds from a preset value and closing when the pressure drops to allowed

value. It is a self-operating valve, therefore no control part is necessary. Pressure relief valves are designed to regulate the fluid flow continuously.

Another alternate device for regulating high pressure is an anticipator relief valve. It is crucial in order to protect pumps, pumping equipment and all applicable pipeline from water hammer pressure peaks caused by the sudden change of flow velocity within a pipeline.

2.5.3. One-way tank

The one-way tank is a storage vessel connected to the hydraulic system. And it has normally closed check valve in the end, which regulate the flow only in one direction (from the tank into the system). An important advantage of the one-way tank rather than a surge tank is that it can have a relatively lower height in the vessel thus more compact design [8].

2.5.4. Velocity profile

The water hammer effect can be reduced with lower velocity of the fluid in the pipeline [9]. However, it is given in the manual of the system that the minimum velocity of the slurry should be 1.2 m/s [10]. But in a place where water hammer takes place, it should be reduced up to the minimum, decreasing the water hammer effect.

Table 1. Primary attributes and decision variables of the water hammer protection devices. [11]

Protection Approach	**Primary Attributes**	**Decision Variables**
Check valve	Limits flow to one direction Permits selective connections Prevents/limits line draining	Size and location Specific valve configuration Antishock (dampening) characteristics
Pump bypass line	Permits direct connection and flow around a pump Can limit up-and-down surge	Size and location Exact points connected Check-valve properties
Open surge tank	Permits inflow/outflow to external storage May require water circulation Can limit up-and-down surge	Size and location Connection properties Tank configuration Overflow level
Closed surge tank (air chamber)	As pressure changes, water exchanged so the volume of	Location Volume (total/water/air) Configuration/geometry

	pressurized air expands or contracts Needs compressor	Orifice/connector losses
Feed tank (one-way tank)	Permits inflow into the line from an external source Requires filling	Size and location Connection properties Tank configuration
Surge anticipation valve	Permits discharge to a drain Has both high- and low-pressure pilots to initiate action May accentuate down the surge	Size and location High-and low- pressure set points Opening/closing times
Combination air-release and vacuum-breaking valve	When the pressure falls, large orifice admits air Controlled release of pressurized air through an orifice	Location Small and large orifice size Specific valve configuration
Pressure-relief valve	Opens to discharge fluids at a preset pressure valve Generally opens quickly and closes slowly	Size and location High-pressure set point Opening/closing times

2.6. Pinch valve

Lime slurry is slightly abrasive and it has a high tendency to build-up scale, thus it is recommended to use a pinch valve for transporting lime with through the pipeline. When elastomer sleeve changes its shape in order to open and close, it breaks down the scale allowing them to pass through. Rubber sleeve in the pinch valve let the abrasive particle bounce off the surface, therefore reducing wear. Only the sleeve of the pinch valve is in contact with the medium (milk of lime) meaning that simply changing the sleeve result in perfectly functioning pinch valve.

In the system, pinch valves are used for controlling flow from the main line to the distributed units. They are driven by pneumatic cylinders pinching the flexible sleeve from both sides to close or releasing it to open. Pneumatic cylinders are automatically controlled by the pH value in the system. They are suited for slurry flow because, in open state, it is smooth and identical to the normal pipeline (no concave space for the slurry to accumulate) [12].

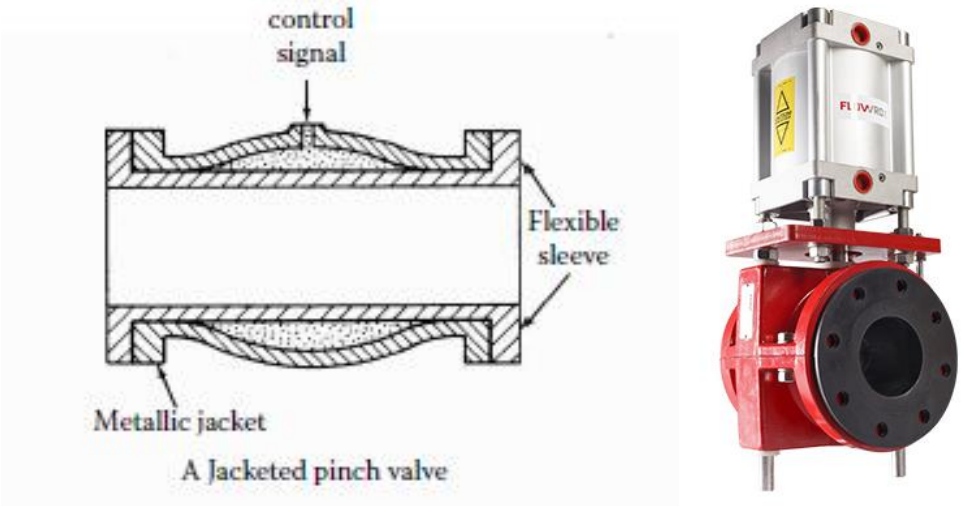

Figure 2.2. Pneumatic driven pinch valve [13]

2.7. Piping network

As mentioned earlier, branched pipeline systems have weaker water hammer effect compare to a simple linear system. The valve is located in the branched pipeline as shown.

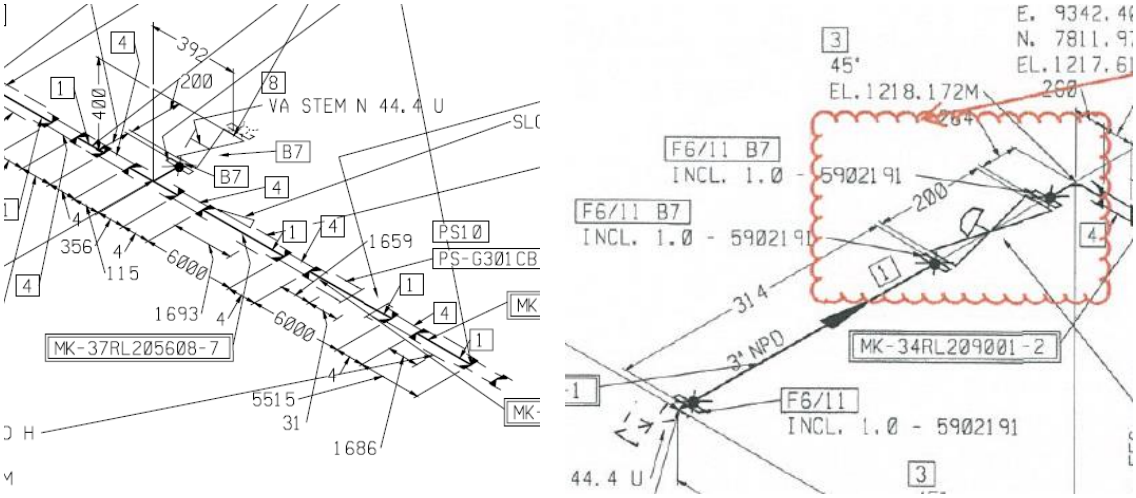

Figure 2.3. Isometric drawing pinch valve in the piping network [14], [15]

A distribution line is branched from the main line with a particular angle going up and equipped with pneumatic pinch valve (framed in red curvatures) as well as a manual pinch valve. The diameter of the main pipe is 6” and branched distribution pipe diameter 3”. It is essential for the valve to be located in a vertical or sloped pipeline rather than a horizontal pipe, allowing the build-up scale to fall due to gravitation.

2.8. Lime specification

Lime is a critically important part of the operation and on average, they use 18600 ton to 43800 ton per annum (50 – 120 ton per day). Some required properties are given in the tables below.

Table 2. Physical properties of lime

Bulk Density	Crushed
(kg/m3)	1070-1170
(lbs/ft3)	67-73
Slaking rate	
1. Temperature rise in 30 sec (°C)	41
2. Temperature rise in 3 min (°C)	50
3. Total Temperature rise (°C)	55
4. Total active slaking time (minutes)	3
Particle Size Distribution	100% -1.5 mm

Table 3. Classical Reference Data

Specific Gravity	3.0 – 3.4
Solubility in water (10°C)	1.31
pH (saturated solution (25°C)	12.4

Table 4. Chemical properties

Available lime as calcium oxide (CaO)(%)	> 85
Magnesium oxide (MgO) (%)	< 1.5
Silica / Silicon dioxide (SiO_2) (%)	< 2.0
Ferric oxide (%)	< 0.5
Alumina (Al_2O_3) (%)	< 0.5
Total sulphur (S) (%)	0.02
Loss on ignition (%)	< 2.5
Carbonates ($CaCO_3$)(%)	< 3.5

3. Milk of lime flow simulation

In this study, lime slaking and distribution system at Oyu Tolgoi LLC is studied using Wanda 4.5 Engineering software on various closure rate for different valves. Physical characteristics of milk of lime and pipeline material should be either calculated or determined by experiment.

3.1. Determination of properties

3.1.1. Determination of fluid properties

One of the important characteristics of the slurry is viscosity or relative viscosity. There are few empirical models which are proven to be practical as in [16], [17], [18], [19]. And Liu's model for predicting relative viscosity is the most accurate among the others for the milk of lime [20].

The Liu's Model for predicting relative viscosity of the slurry

$$\eta_r = [c \cdot (\phi_m - \phi)]^{-n} \tag{16}$$

where η_r = relative viscosity, nu

c = 2.3561 (constant from Liu's model)

ϕ_m = 0.504 (maximum solid concentration)

ϕ = solid concentration, vol. %

n = 2 (flow dependant parameter and suspension specific)

$$\eta_r = \frac{\mu_{slurry}}{\mu_{liquid}} \tag{17}$$

$$\phi = \frac{V_s}{V_s + V_l} \tag{18}$$

where V_s = solid volume, m^3

V_l = volume of the liquid, m^3

μ_{slurry} = dynamic viscosity of the slurry, $\frac{kg}{m \cdot s}$

μ_{liquid} = dynamic viscosity of the liquid, $\frac{kg}{m \cdot s}$ (water)

As observed in [20], slurries with solid concentration up to 37.8 vol.% (approximately 40.5 mass.%) show Newtonian behavior while slurries with more solid volume concentration show pseudoplastic nature. Optimally, the concentration of slurry flowing in the pipeline is 20% solid by a mass fraction. Therefore it is safe to consider the slurry as a Newtonian fluid. Assuming the water added to the lime slaker is distilled water with no contamination, the relationship between solid concentration by a mass fraction (χ) and solid concentration by volume fraction can be expressed as follows:

$$\phi = \frac{\chi}{\rho_r - \chi \cdot (\rho_r - 1)} \tag{19}$$

$$\rho_r = \frac{\rho_s}{\rho_l} \tag{20}$$

where ρ_l = 1000 kg/m^3 (liquid density)

ρ_s = 1070 – 1170 kg/m^3 (bulk density of the solid)

Viscosity is a temperature dependent parameter, assuming average temperature in the system is 50°C the calculation of dynamic viscosity is carried out for various solid concentration and it is shown in Table 5. And the parameters at 50°C required for the calculation are listed below. Here the bulk density of the solid is taken as $1120 \frac{kg}{m^3}$ at the average of the given range.

$\mu_w = 0.547 \cdot 10^{-3} \frac{kg}{m \cdot s}$; $\rho_w = 988.02 \frac{kg}{m^3}$; $\rho_r = \frac{\rho_s}{\rho_l} = \frac{1120}{988.02} = 1.134$

Table 5. The relative viscosity of slurry for different solid concentrations

Mass fraction, nu $\frac{m_s}{m_s+m_l}$	Volume fraction, nu $\frac{V_s}{V_s+V_l}$	Relative viscosity, nu
0.150	0.135	1.321
0.155	0.139	1.354
0.160	0.144	1.389
0.165	0.148	1.425
0.170	0.153	1.462
0.175	0.158	1.502
0.180	0.162	1.542
0.185	0.167	1.585
0.190	0.171	1.629
0.195	0.176	1.675
0.200	0.181	1.723
0.205	0.185	1.774
0.210	0.190	1.827
0.215	0.195	1.882
0.220	0.199	1.940
0.225	0.204	2.000
0.230	0.209	2.064
0.235	0.213	2.130
0.240	0.218	2.200
0.245	0.223	2.274
0.250	0.227	2.352

The density of the slurry is required for successful simulation. Thus the density of milk of lime is determined by experiment by varying solid concentration from 15% to 25%. The result of the experiment is in Table 6. Associated graph for slurry density as a function of solid concentration is in Figure 3.1.

Table 6. The density & kinematic viscosity of the slurry depending on solid concentration by mass fraction

Solid concentration, %	Density, $\frac{kg}{m^3}$	Kinematic viscosity, $10^{-6}\frac{m^2}{s}$
15.0	1053.7	0.711
15.5	1057.6	0.726
16.0	1059.6	0.743
16.5	1064.6	0.759
17.0	1069.1	0.775
17.5	1074.2	0.793
18.0	1079.6	0.810
18.5	1084.7	0.829
19.0	1089.5	0.848
19.5	1094.7	0.868
20.0	1099.7	0.888
20.5	1104.9	0.910
21.0	1109.9	0.933
21.5	1115.2	0.957
22.0	1120.5	0.982
22.5	1125.8	1.007
23.0	1131.1	1.035
23.5	1136.4	1.063
24.0	1140.6	1.094
24.5	1145.8	1.125
25.0	1151.0	1.159

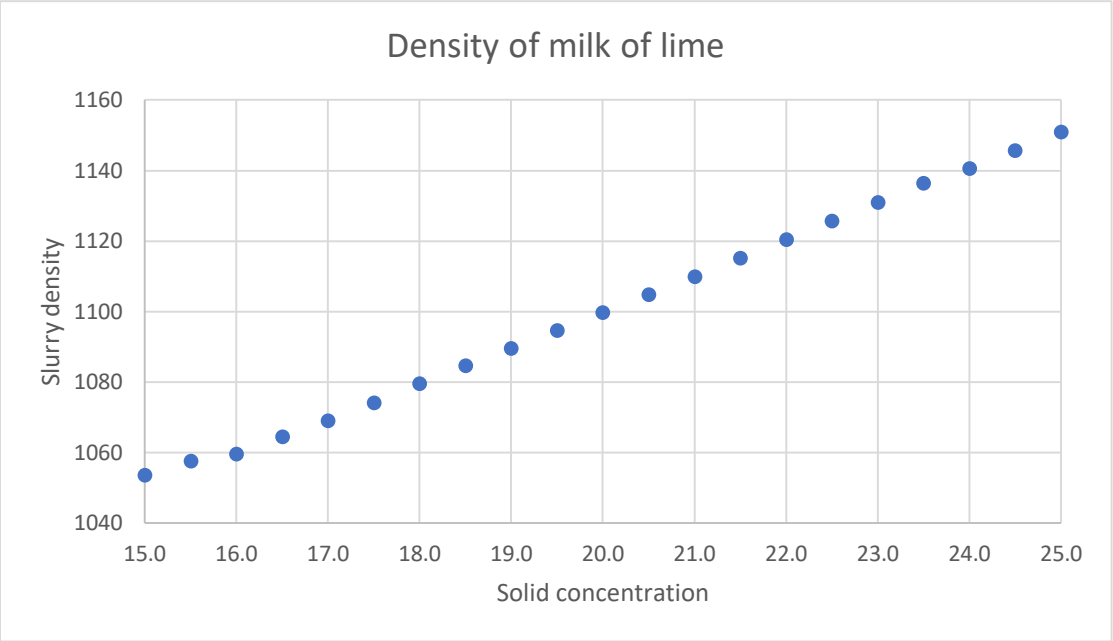

Figure 3.1. Relationship between slurry density and solid concentration

3.1.2. Valve properties

The pinch valve in the system is pneumatic operated valve from Flowrox Flowsys. Inc. as shown in the associated figure below. The sleeve of the valve is made out of natural rubber with an inner bore diameter of 80mm.

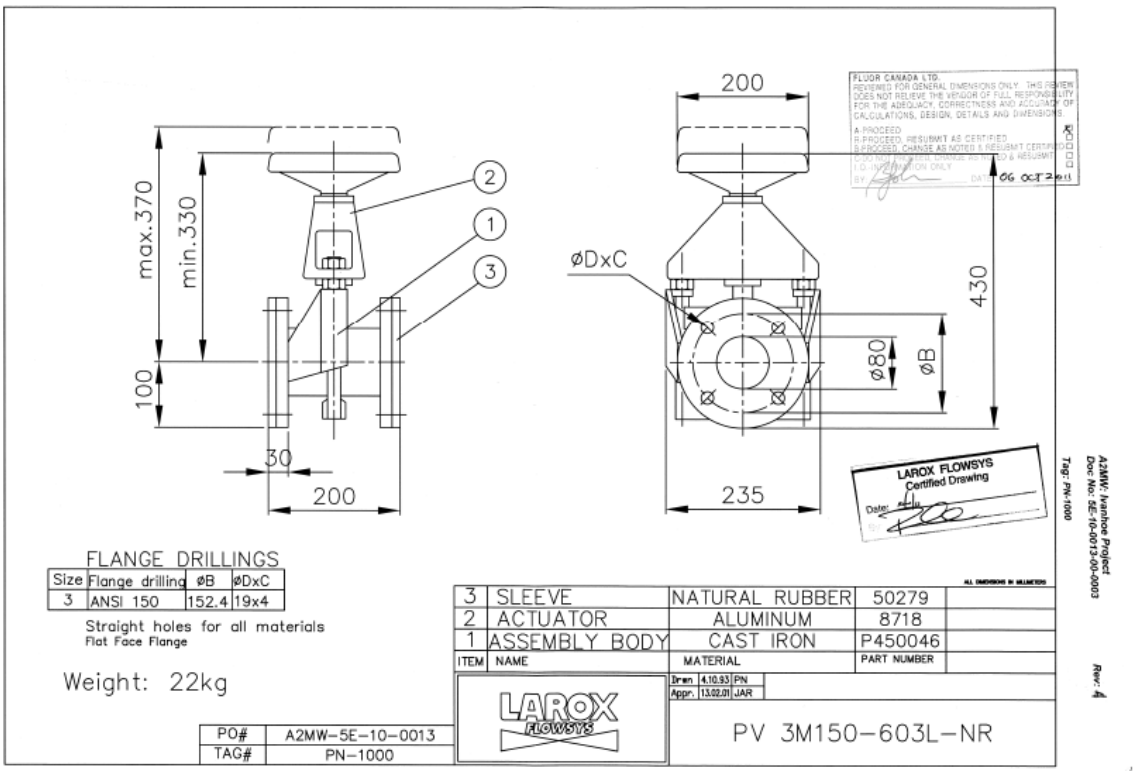

Figure 3.2. Technical drawing of pneumatic operated pinch valve

The effect of water hammer is dependent on valve properties, which can be expressed by flow factor K_v. Flow factor is the flow of water with temperature ranging 5 – 30°C through a valve in cubic meters per hour (m3/h) with a pressure drop of 1 bar and the equation for general scenario is in Eqs. 21., where Δp is a pressure drop across the valve and Q is the volume flow rate .

$$K_v = Q \cdot \sqrt{\frac{\rho}{1000 \cdot \Delta p}} \tag{21}$$

An inherent characteristic curve determines the performance of a valve and it is a plot of a valve position vs. flow factor (K_v) or percentage of maximum K_v. The most common characteristic curves are the quick opening, linear and equal percentage curves (Figure 3.3.(a)). Additionally, there is an installed characteristic curve, which is a plot on the same axis as the inherent characteristic curve. Installed characteristic curve differ from the inherent characteristic curve due to the change in differential pressure across the valve depending on valve position. How the curve shift is affected by the pump characteristic curve and the static and dynamic head in the system [21], an example is shown in Figure 3.3.(b).

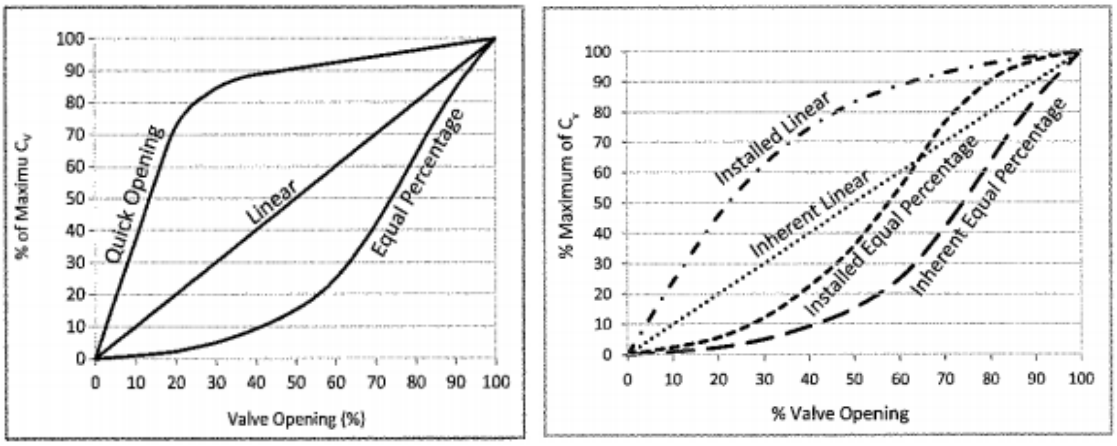

(a) (b)

Figure 3.3. a) Inherent characteristic curve; b) The shift of the inherent characteristic curve

The request for the valve specification was requested to the Flowrox Flowsys. Inc. and C_v values for the valve with various size was sent (see Table 7). C_v values and K_v values are technically the same but expressed in a different unit. An inner bore diameter of the valve is given as 80mm, therefore data at that point is used for the simulation.

Table 7. Flowrox valve C_v values

		Valve size, mm										
		25	32	40	50	65	80	100	125	150	200	250
Valve opening,%	0	0	0	0	0	0	0	0	0	0	0	0
	10	10	16	25	39	65	98	154	241	347	616	963
	20	24	39	61	96	162	246	384	601	865	1537	2402
	30	40	66	103	162	273	414	647	1010	1455	2586	4042
	40	57	93	145	226	382	579	905	1414	2037	3621	5657
	50	72	116	181	284	479	725	1134	1772	2552	4536	7099
	60	82	135	211	329	557	843	1317	2059	2964	5270	8234
	70	90	148	232	362	612	927	1448	2263	3258	5792	9050
	80	95	156	244	381	645	976	1525	2384	3432	6102	9534
	90	96	157	248	388	657	994	1554	2428	3497	6216	9713
	100	96	158	248	388	657	994	1554	2428	3497	6216	9713

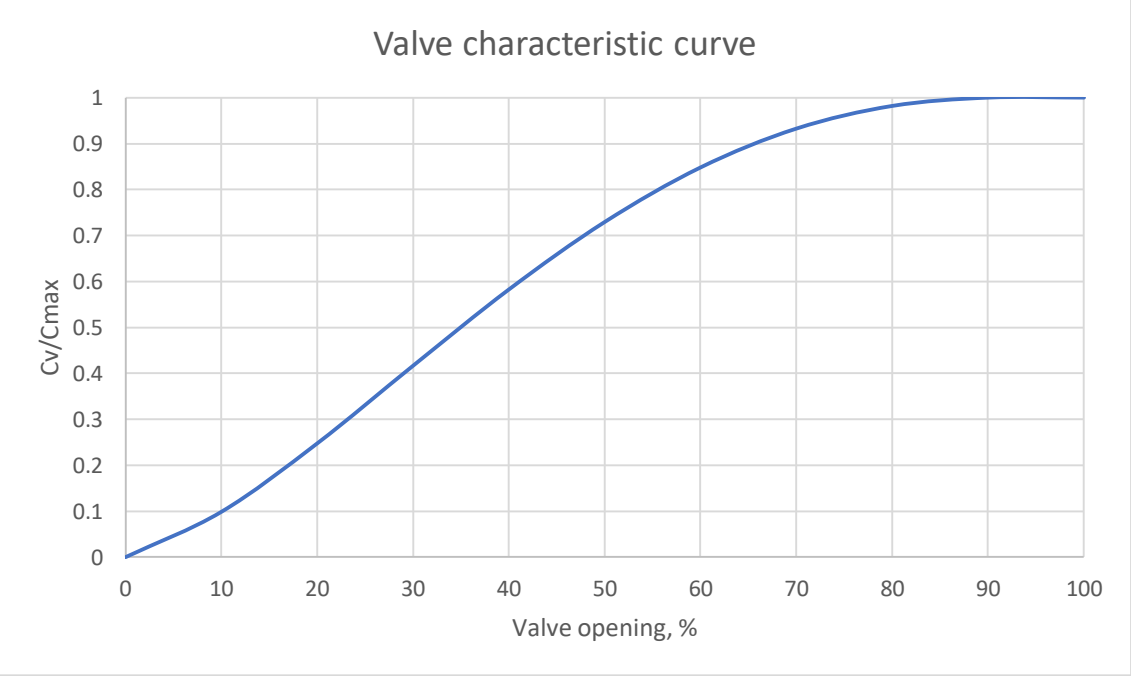

Figure 3.4. The characteristic curve of a valve with 80mm diameter

3.1.3. Properties of pipe material

A53 Grade B as defined from ASTM (American Society for Testing and Materials) carbon steel is used for the pipe. ASTM specification A53 covers seamless and welded, black and hot-dipped galvanized nominal (average) wall pipe for coiling, bending, flanging and

other special purposes. Grade B is one of the most spread out material to be used for steel pipelines, it can be found in mechanical, pressure application and is acceptable for ordinary uses in steam, water, gas, and air lines. According to ASTM data, physical and chemical properties are given in Table 8 - 10.

Table 8. Chemical properties of ASTM A53-B Gr B.

Chemical composition	Grade A	Grade B
Carbon, max. %	0.250	0.300
Manganese, %	0.950	1.200
Phosphorous, max. %	0.050	0.050
Sulfur, max. %	0.045	0.045
Copper, max.%	0.400	0.400
Nickel, max. %	0.400	0.400
Chromium, max. %	0.400	0.400
Molybdenum, max. %	0.150	0.150
Vanadium, max. %	0.080	0.080

Table 9. Mechanical properties of ASTM A53-B Gr B.

Yield Strength, MPa	Ultimate Strength, MPa	Young's Modulus, GPa	Poisson's ratio	Hoop Modulus, GPa	Shear Modulus, GPa
241.3	413.7	200	0.3	200	80

Table 10. Pipe thickness at schedule number 80

Nominal Pipe size	O.D.	Schedule number	Wall thickness, inches	Wall thickness, mm
3"	3.5"	80	0.3	7.62
6"	6.625"	80	0.432	10.9728

It is common for the milk of lime to be transported in a pipe with schedule number 80 and the table above has been sent from the organization.

3.2. Simulation set-up on Wanda Engineering 4.5

3.2.1. A brief introduction to simulation software

Wanda is a software specialized in hydraulic systems, produced by Deltares Institute in Netherland. Deltares is an independent institute for applied research in water and subsurface, they work mostly focusing on deltas - densely populated and vulnerable coastal areas as well as river basins.

One of their product is Wanda Engineering 4.5, which used mainly for:

- Pump & Line sizing
- Flow distribution
- Pressure surge analysis (water hammer)
- Operational control
- Heat transfer analysis etc.

In order to carry out the simulation, the free trial version with a one-month valid license was requested from the institute and they approved the request. It can simulate the steady-state case as well as transient scenarios as well. It has many features including pump, pipe, air vent, surge tank as well as control devices.

3.2.2. Flowing media

For successful simulation, it is required to insert properties of the fluid as well as the pipeline system and component specification.

The software is capable of carrying out simulation in Newtonian fluid as well as slurry fluid. However, the slurry flow simulation required the yield stress and bulk modulus of the media in addition to viscosity, density, and vapor pressure which are required properties for the Newtonian flow. According to other researches [20], it is proven to show Newtonian behavior up to a solid concentration of 40.5%, it can be simplified as a Newtonian fluid.

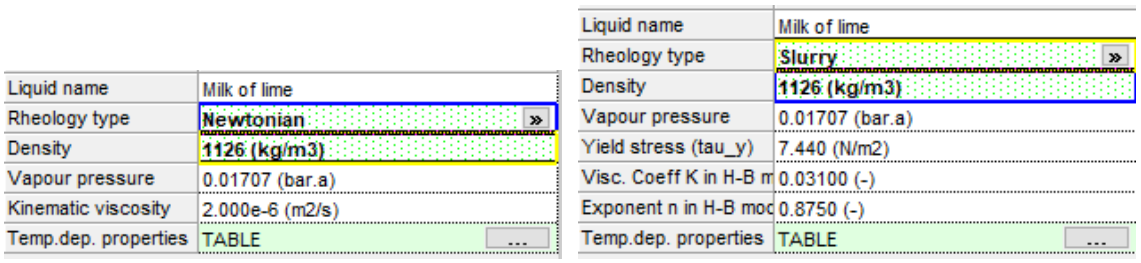

Figure 3.5. Fluid window on Wanda 4.5

Values for viscosity and density are taken from Table 3 & 4. Vapour pressure of the slurry is assumed to be the same as the water vapor pressure due to water is most likely to evaporate during pressure drop and the solid particles will settle.

3.2.3. Pump set-up

There are several ways to simulate fluid flow in Wanda including pump, tank with constant discharge, head and pressure. From the manufacturer following QHE diagram was sent and it is given into the simulation as a table shown in Table 11. The software calculates the power from given discharge, pump head, and efficiency. There is a small difference in power between the calculated power value in Wanda and power specified from the manufacturer. But the difference is negligible and it will not affect the simulation result. At the mine, the pump work at a discharge rate of 180 m^3/h and discharge pressure of approximately 5 bar. Simulation is set for a constant discharge rate.

Table 11. QHE characteristic of the pump in Wanda

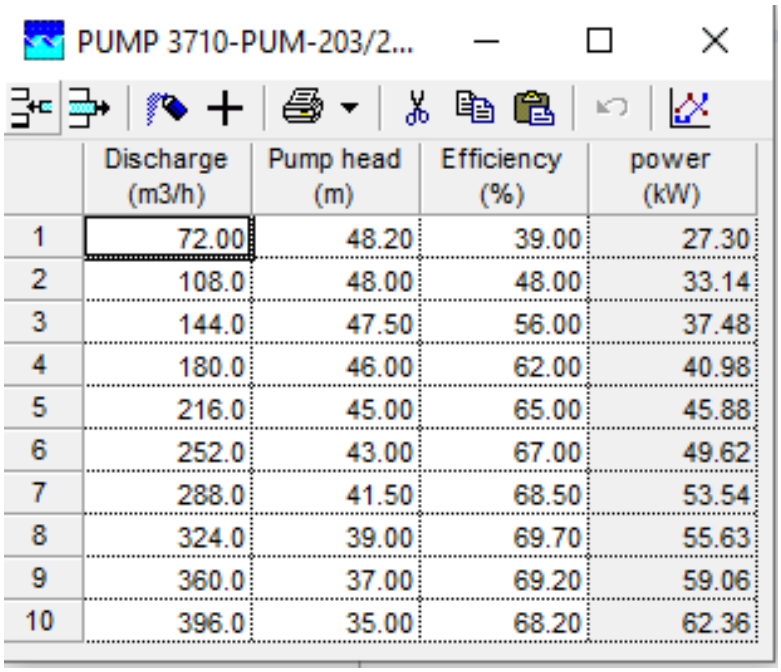

	Discharge (m3/h)	Pump head (m)	Efficiency (%)	power (kW)
1	72.00	48.20	39.00	27.30
2	108.0	48.00	48.00	33.14
3	144.0	47.50	56.00	37.48
4	180.0	46.00	62.00	40.98
5	216.0	45.00	65.00	45.88
6	252.0	43.00	67.00	49.62
7	288.0	41.50	68.50	53.54
8	324.0	39.00	69.70	55.63
9	360.0	37.00	69.20	59.06
10	396.0	35.00	68.20	62.36

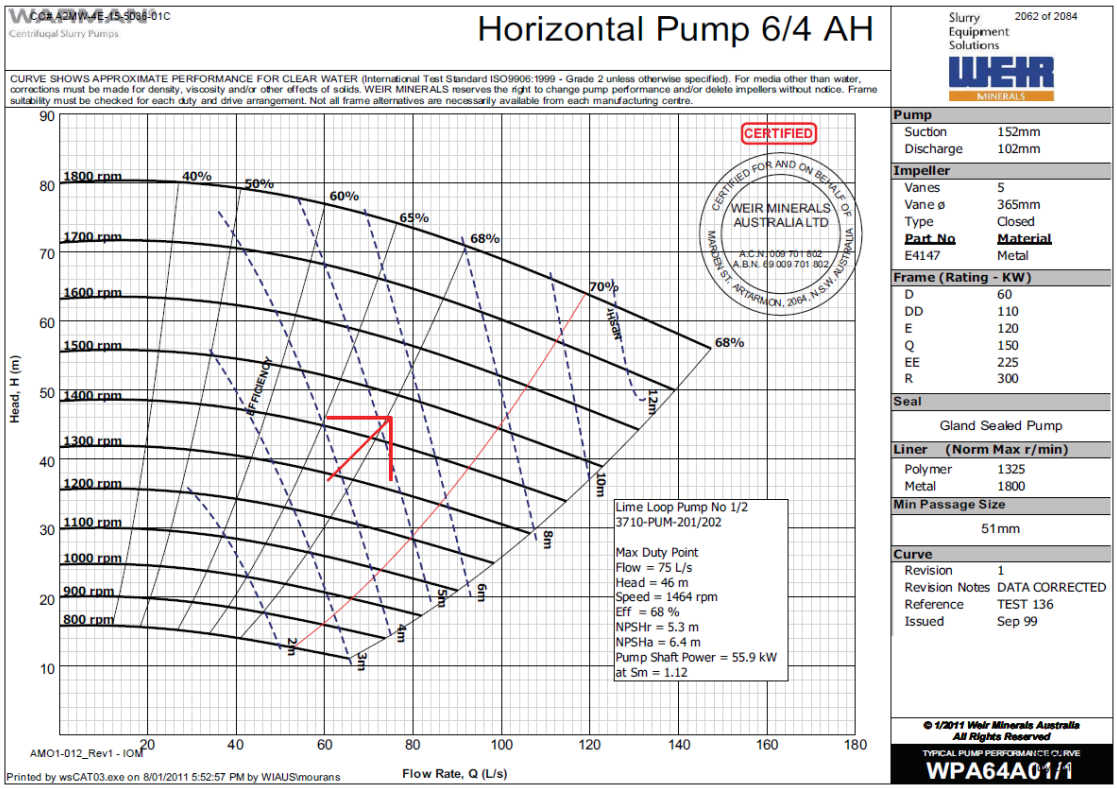

Figure 3.6. Pump QHE diagram

3.2.4. Equivalent pipeline system

Isometric drawing of the system was given and it is translated to Wanda taking the origin of the coordinate at the beginning of the pipe (outlet of the pipe). For Wanda Engineering 4.5, it is possible to set-up the geometry of the pipeline in several ways. For this particular simulation, “xyz” mode is used, and the pipeline profile is shown below. Only part of the system is precisely illustrated from isometric drawing 3710-RL2056-C1B-01_1 to 3710-RL2056-C1B-01_8 and 3430-RL2095-C1B-01_1. And the rest of the system is not prior for the simulation, therefore, it is simplified. Minor losses such as elbows and fitting are neglected. In the figure below, the pipe profile is shown as well as other specifications of the pipeline that are required. Friction loss is calculated using the Darcy-Weisbach model. There is another pipe right in front of the valve, which is relatively very short (~0.9m) and also translated from the isometric drawing taking the manual operated valve as part of the pipe (when it is open it does not affect any process in the system).

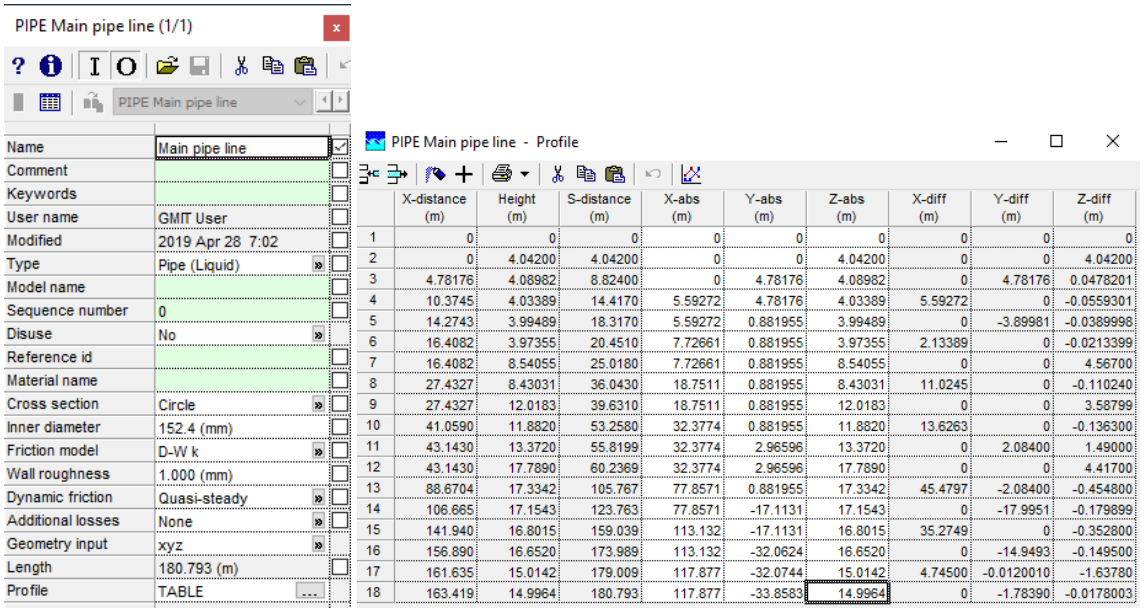

	X-distance (m)	Height (m)	S-distance (m)	X-abs (m)	Y-abs (m)	Z-abs (m)	X-diff (m)	Y-diff (m)	Z-diff (m)
1	0	0	0	0	0	0	0	0	0
2	0	4.04200	4.04200	0	0	4.04200	0	0	4.04200
3	4.78176	4.08982	8.82400	0	4.78176	4.08982	0	4.78176	0.0478201
4	10.3745	4.03389	14.4170	5.59272	4.78176	4.03389	5.59272	0	-0.0559301
5	14.2743	3.99489	18.3170	5.59272	0.881955	3.99489	0	-3.89981	-0.0389998
6	16.4082	3.97355	20.4510	7.72661	0.881955	3.97355	2.13389	0	-0.0213399
7	16.4082	8.54055	25.0180	7.72661	0.881955	8.54055	0	0	4.56700
8	27.4327	8.43031	36.0430	18.7511	0.881955	8.43031	11.0245	0	-0.110240
9	27.4327	12.0183	39.6310	18.7511	0.881955	12.0183	0	0	3.58799
10	41.0590	11.8820	53.2580	32.3774	0.881955	11.8820	13.6263	0	-0.136300
11	43.1430	13.3720	55.8199	32.3774	2.96596	13.3720	0	2.08400	1.49000
12	43.1430	17.7890	60.2369	32.3774	2.96596	17.7890	0	0	4.41700
13	88.6704	17.3342	105.767	77.8571	0.881955	17.3342	45.4797	-2.08400	-0.454800
14	106.665	17.1543	123.763	77.8571	-17.1131	17.1543	0	-17.9951	-0.179899
15	141.940	16.8015	159.039	113.132	-17.1131	16.8015	35.2749	0	-0.352800
16	156.890	16.6520	173.989	113.132	-32.0624	16.6520	0	-14.9493	-0.149500
17	161.635	15.0142	179.009	117.877	-32.0744	15.0142	4.74500	-0.0120010	-1.63780
18	163.419	14.9964	180.793	117.877	-33.8583	14.9964	0	-1.78390	-0.0178003

Figure 3.7. Pipeline profile on Wanda

A T-Junction is placed after the main valve and from there the distribution line transport the slurry to the unit. The end of the line is open, therefore, “Tap non-return flow” is used concerning that it should not flow back (see Figure 3.8.).

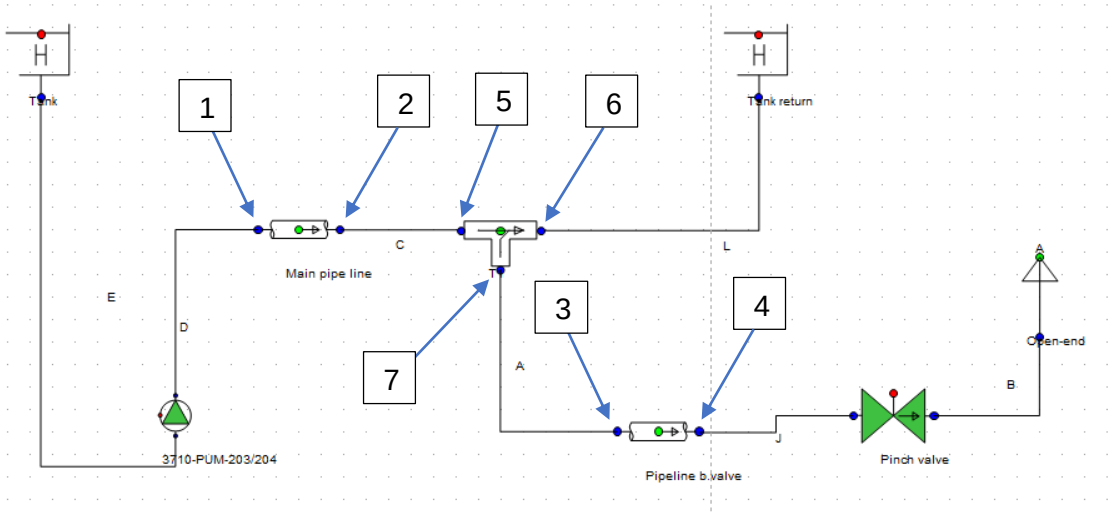

Figure 3.8. Illustration of the system on Wanda

3.3. Dependent and independent variables

As independent variables, valve closure rate, valve type, presence of protective devices, and solid concentration of the slurry are considered. The dependent variable is the water hammer effect, mostly the pressure peaks.

The valve can be closed at different rates with different profiles, for example in some researches, they recommend to close the valve rapidly at the beginning and slowly as the valve opening decreases [22]. Thus, it may be worth varying this variable

4. Results and Discussions

4.1. Steady-state flow simulation

For the steady-state, the valve is 100% and the pressure right after the pump is 5.363barg (gauge pressure in bar). The pressure is decreasing continuously due to pressure loss in the pipe. At the point where it is increasing, the equivalent piezometric head drop is less than geometrical head drop, therefore it can gain some energy caused by gravitation.

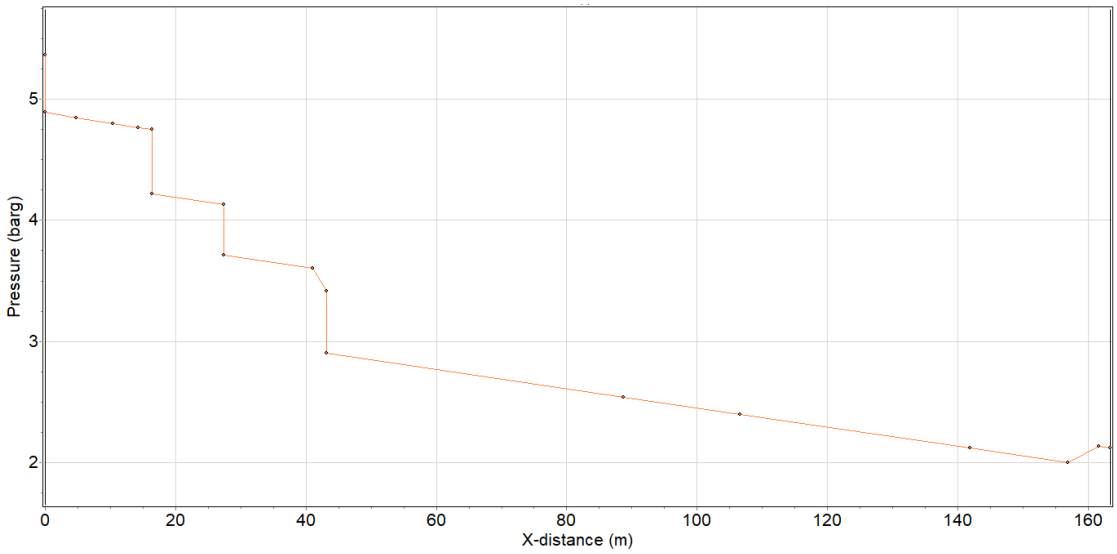

Figure 4.1. Pressure profile along the main pipeline

4.2. Transient flow simulation

For the general transient flow simulation, the valve will close in 5 seconds with uniform closure rate, pinch valve with 80mm inner bore diameter is used and no protective device is present in the system. In the first 3 seconds, the valve is still 100% open, it helps the comparison between steady-state flow profile and transient flow profile. Overall the simulation is done for 20 seconds, assumed to be enough time for the system to stabilize yet not that much time for the computer to jam. Time step for the simulation is 0.001s, thus it can provide a more accurate result. The fluid is at 20 % mass concentration and viscosity and density of the fluid is set as $\rho = 1099.7\ \frac{kg}{m^3}$, $\nu = 0.888 \cdot 10^{-6}\ \frac{m^2}{s}$.

Transient flow simulation provides pressures at the end of the drawn pipes, discharge rates at the T-junction and valve, pressure right before the valve and right after the valve as well. Points for the pressures are illustrated in Figure 3.7. and the following descriptions are placed below the graph.

- Pressure 1 (Centreline) PIPE Main pipe line – Pressure at the point 1
- Pressure 2 (Centreline) PIPE Main pipe line – Pressure at the point 2
- Pressure 1 (Centreline) PIPE Pipeline b.valve - Pressure at the point 3
- Pressure 2 (Centreline) PIPE Pipeline b.valve - Pressure at the point 4
- Discharge 1 T-JUNC T1 – Discharge flow rate at point 5
- Discharge 2 T-JUNC T1 – Discharge flow rate at point 6
- Discharge 3 T-JUNC T1 – Discharge flow rate at point 7 (negative due to the opposite flow direction of the T-junction that was available)

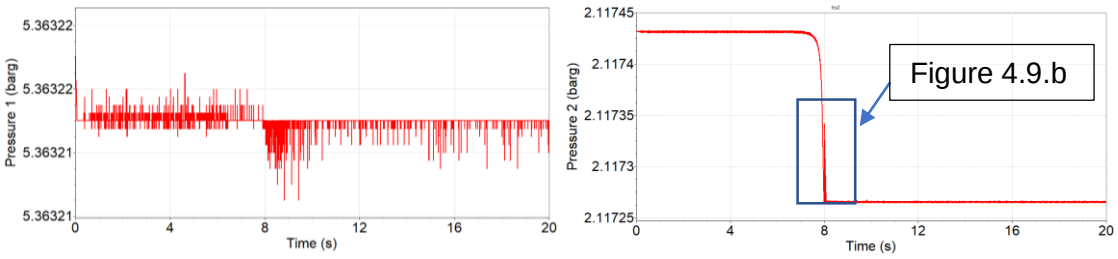

Figure 4.2. Pressure profile at point 1 & 2

As shown in Figure 4.2., the main pipeline pressure change is not significant, it is in order of 0.00001barg, thus it does not have a big impact. The flow in the main pipeline is considered to be turbulent flow, therefore pressure is not linear it is oscillating with insignificant amplitude. However, in the pipe right before the valve, the pressure change is relatively high (see Figure 4.3.). Also in this pipe, the velocity is lower thus it is more of a laminar flow than turbulent flow.

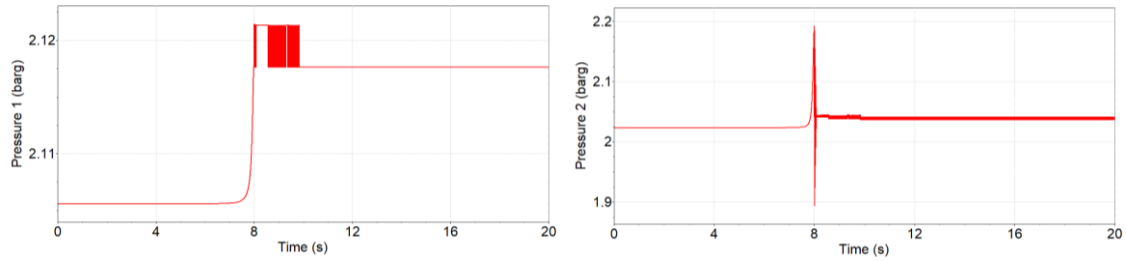

Figure 4.3. Pressure profile at point 3 & 4

For the pressure at point 3, the pressure increases with a maximum of 0.016barg, from there the pressure oscillates from time to time showing transitional flow behavior. It is

caused by entering fluid into the pipe and reflecting back from the valve into the main pipeline.

The pressure at point 4 starts changing at 7.5 seconds and from there it increases rapidly in the magnitude of 0.2barg (about 10% of the pressure at this point for steady-state), which is relatively high compared to the pressure change in pressure at point 1, 2 & 3. It rapidly damps in about 0.2 seconds, leaving turbulent flow behind with slightly higher pressure than the pressure in steady-state. The flow circulates even after the valve is closed, it prevents the fluid from settling.

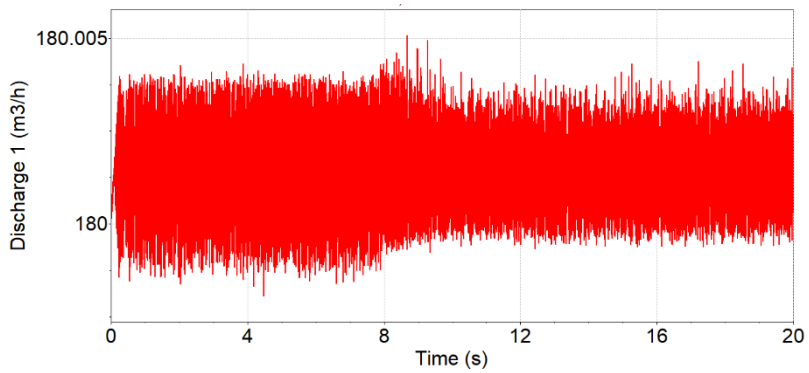

Figure 4.4. Volumetric flow rate entering the T-junction at point 5

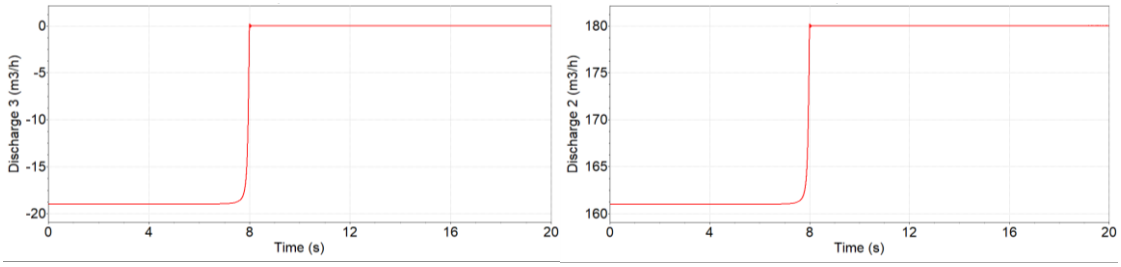

Figure 4.5. Volumetric flow rate exiting the T-junction at point 6 & 7

As given by the initial condition, at t = 0s the Discharge 1 is 180 m^3/s and it is reducing and increasing insignificantly ranging in the range of 180.005 m^3/s and 179.997 m^3/s. This is related to the turbulence of the flow as well as the position of the valve. When the valve is closed the flow rate increases, it may be caused by dissipation of pressure loss on the T-junction.

In Figure 4.5., the discharge profiles of point 6 & 7 show identical properties, because the flow rate passing through the valve decreases as it closes and the decreased flow rate will add into the flow rate passing through point 7. Volumetric flow rate passing through the valve is illustrated as it is increasing, but it is a diversion from the direction of the flow as explained earlier. Since they show the exact same relationship, from this point on only one of it is considered for the comparison.

When we zoom into the discharge profile, an interesting scenario can be observed, the discharge rate is showing damping oscillation right after the moment of full closure of the valve (see Figure 4.6.).

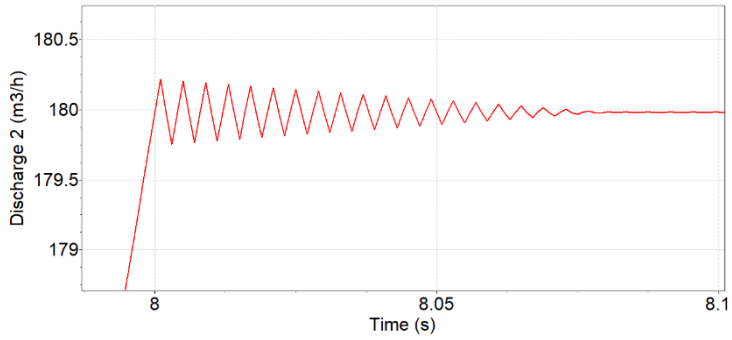

Figure 4.6. Damping oscillation of discharge rate at point 6

4.3. Transient flow with different types of valve

4.3.1. Gate valve

Standard gate valve with an inner diameter of 80mm is specified for the simulation. Unlike pinch valve, the gate valve closes asymmetrically from the top to the bottom and the gate of the valve can wear out easily considering abrasive slurry that is flowing. A typical gate valve design is illustrated in the following figure. A gate valve can easily be automated thus if it has advantages over the pinch valve that is being used in the system, an alternative option can be a gate valve. It starts closing at t = 3s, fully closes at t = 8s.

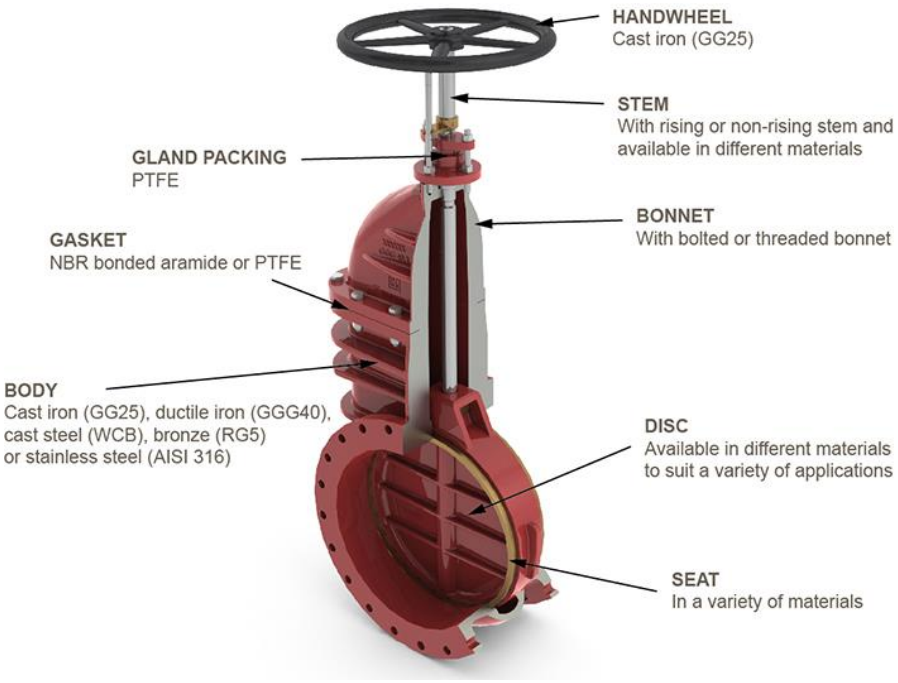

Figure 4.7. A typical gate valve (manually operated)

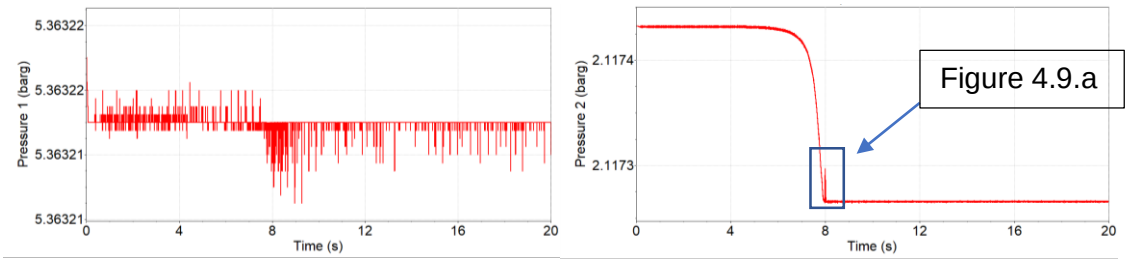

Figure 4.8. Gate valve: Pressure profiles at point 1 & 2

There is no big difference in terms of pressure profile in the main pipeline, except for the small damping oscillation in pressure right after the valve full closure. For the transient flow with the pinch valve, the magnitude was approximately twice as high. The comparison is shown in Figure 4.9. It shows many other different properties such as total time for the oscillation to damp and the geometry of the oscillation.

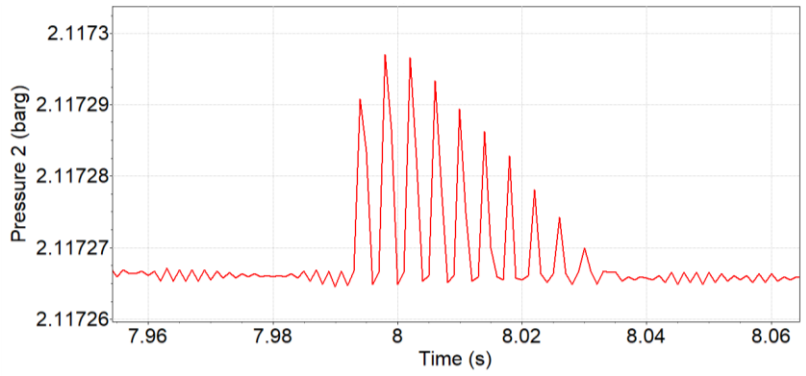

a) Pressure profile at point 2 with a gate valve

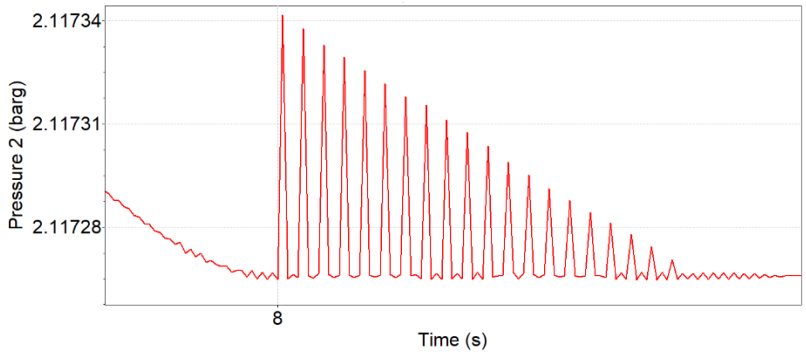

b) Pressure profile at point 2 with pinch valve

Figure 4.9. Contrast between the pressure profiles at point 2 with a gate valve and a pinch valve

Due to the asymmetric closing of the valve, the pressure change at point 3 & 4 simulated as shown in the following figures. The pressure at point 4 starts increasing slowly when the valve opening reduces the pressure increases rapidly in a small amount of time. The maximum pressure change is slightly higher compared to that of the system with the pinch valve. Similarly, the pressure damps and settles at a higher point after the valve is fully closed.

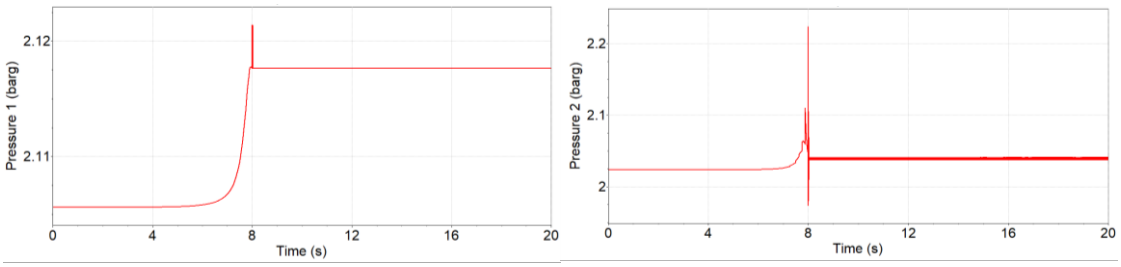

Figure 4.10. Gate valve: Pressure profiles at point 3 & 4

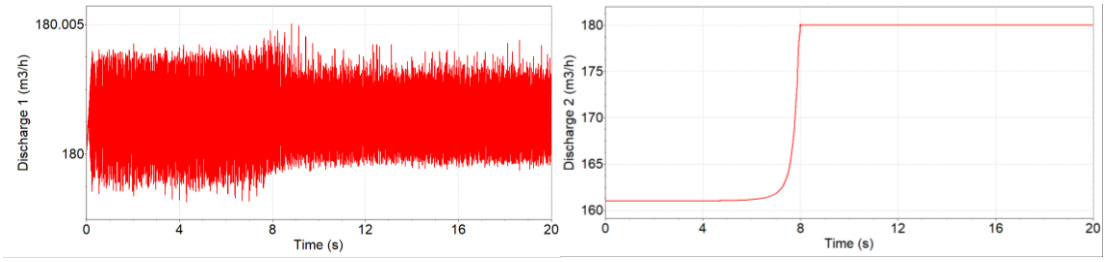

Figure 4.11. Gate valve: Discharge flow rate through point 5 & 7

In general, the relationship between discharge flow rates at T-junction match with the previous results of the system with the pinch valve. Nonetheless, if we zoom into the discharge flow rate through point 7, it deflects at some points and also has very small damping oscillation which is evident in Figure 4.12. The oscillation is damping similar to the first simulation result, but the shape and amplitude of the oscillation differ, it starts 0.01s before the full closure of the valve and slowly shut.

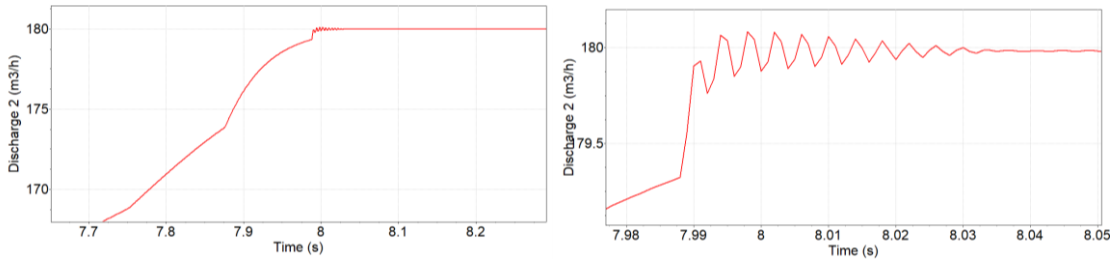

Figure 4.12. Gate valve: Discharge flow rate profile at point 7 (zoomed)

4.3.2. Butterfly valve

A butterfly valve is also compatible for the purpose, the main difference between butterfly valve and the pinch valve (also gate valve) is a butterfly valve start closing from the center meaning that fluid flows closer to the pipe wall when it is partially closed. It can be operated manually, electronically as well pneumatically, the next figure shows a common structure of a manually operated butterfly valve. For the simulation standard butterfly valve with an inner diameter of 80 mm is specified. The valve is open in the first 3 seconds and uniformly close in 5 seconds the same as the previous simulations.

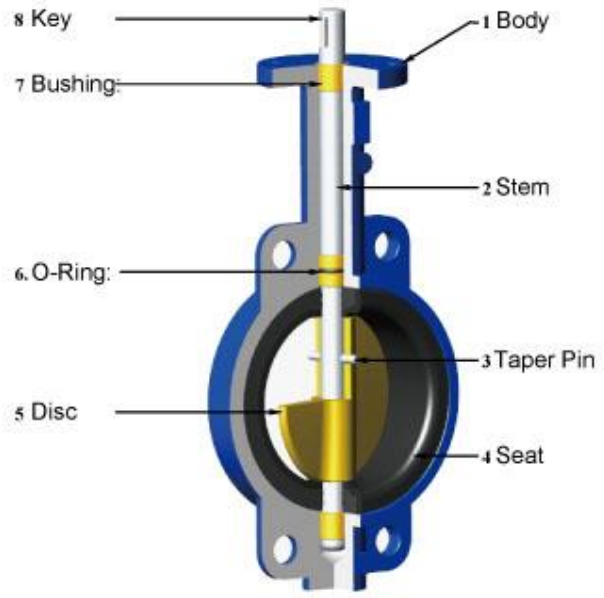

Figure 4.13. A common manually operated butterfly valve [23]

The pressure at point 1 looks identical to previous results as seen in Figure 4.14., so the closure of the valve has a very insignificant effect on the beginning of the main pipeline. At point 2, the pressure profile has no small damping oscillation, unlike the previous two simulation results.

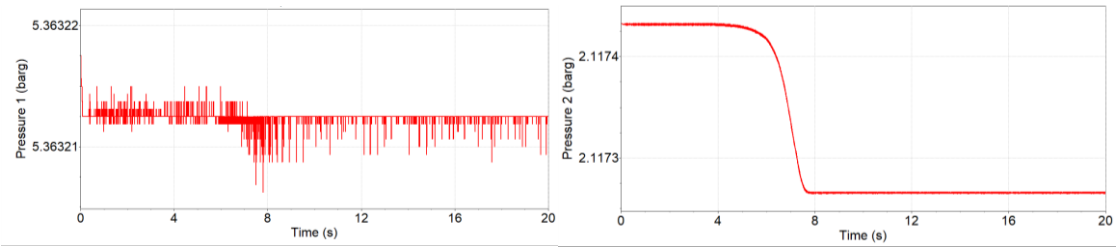

Figure 4.14. Butterfly valve: Pressure profiles at point 1 & 2

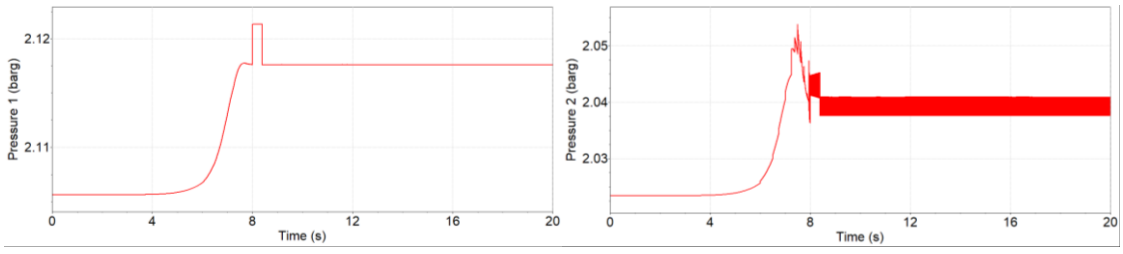

Figure 4.15. Butterfly valve: Pressure profiles at point 3 & 4

An interesting result can be seen from Figure 4.15., the pressure at point 3 was oscillating starting from 8 seconds (right after the full valve closure) in simulation result with a gate

valve as well as a pinch valve. There is no oscillation in pressure only one nonperiodic square wave, it is unusual in comparison to the other ones.

At point 4, the pressure increases from the very beginning of the valve closure and the pressure peaks at t = 7.5 s and slowly shutting up to the point t = 7.95s. From that point, another oscillation starts and again one more starts after valve full closure. Figure 4.16. shows a very complicated combination of oscillation in pressure profile at point 4.

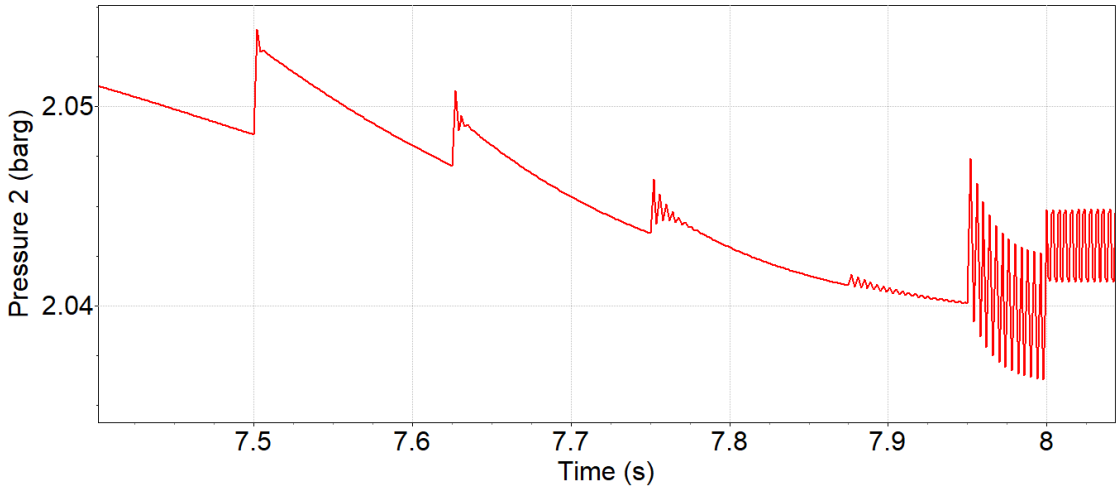

Figure 4.16. Butterfly valve: Pressure profile at point 4 (zoomed)

For the butterfly valve, the pressure increase at point 4 is evidently less than that of the pinch valve and the gate valve. It is increasing from ~2.033 barg up to ~2.055 barg, and for the other two simulations, it was increasing from ~2.033 barg up to ~2.28 barg. One more important thing to note is that the pressure at point 4 does not decrease from its steady-state pressure, this property can be essential when the damage from low pressure is threatening that high pressure such as column separations.

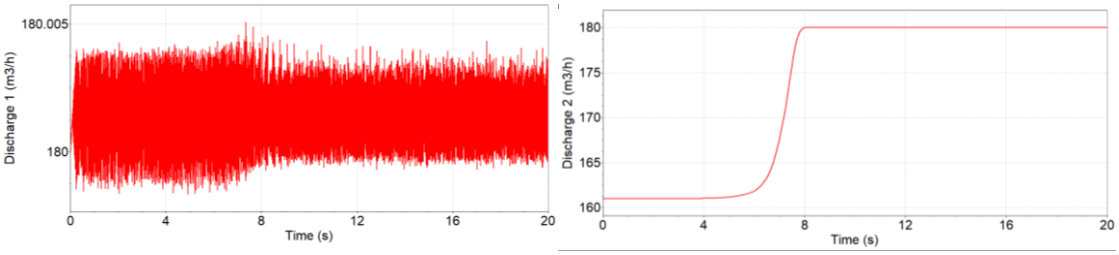

Figure 4.17. Butterfly valve: Discharge flow rate at point 5 & 6

Butterfly valve closure causes a very smooth change in pressure and discharge flow rate. It is related to the centered closure start. In the center of the pipeline, fluid has the highest velocity, and when the valve closes from the center the fluid flow shift causing very smooth and steady change.

4.3.3. Ball valve

A ball valve controls the flow in the conduit using a hollow ball when the opening in the ball is parallel to the pipe, the fluid flows and it closes by turning the ball. Typical ball valve scheme can be seen below. It is also suitable for the purpose, the ball can be made out of many materials and in some milk of lime suspension system, it is used.

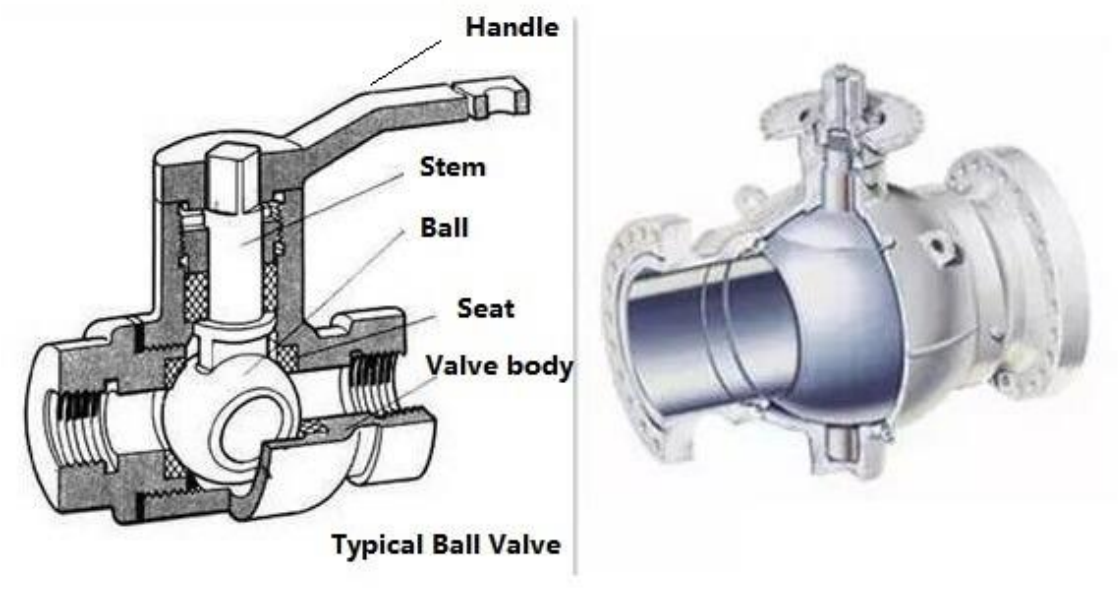

Figure 4.18. Ball valve [24]

Every set-up on the simulation is the same except for the valve type, the valve is specified as a standard ball valve with 80mm inner diameter. Technically, it is similar to the gate valve.

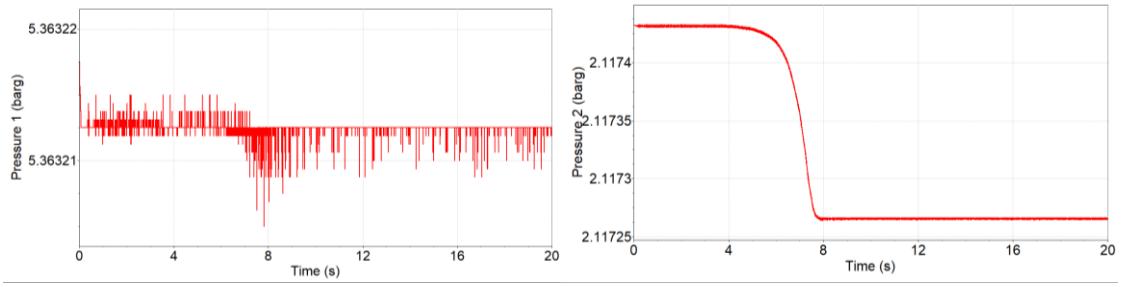

Figure 4.19. Ball valve: Pressure profiles at point 1 & 2

The pressure profile at point 1 is as expected and at point 2 it shows a similar pattern as that of the system with butterfly no damping oscillation right after the valve closure and very smooth pressure drop over time.

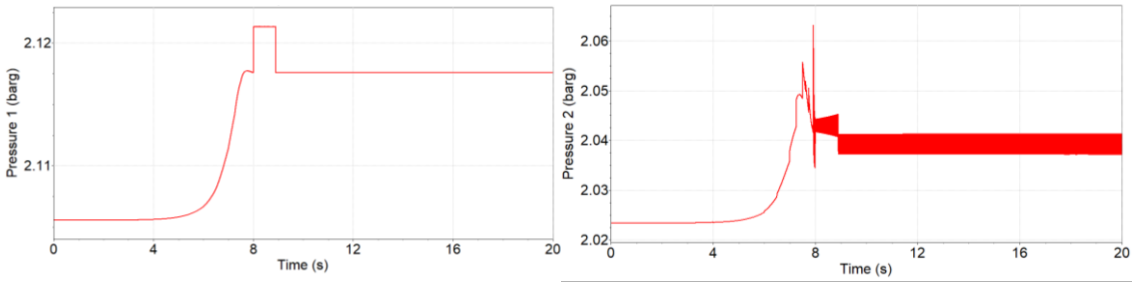

Figure 4.20. Ball valve: Pressure profiles at point 3 & 4

Surprisingly, pressure profiles at point 3 & 4 resemble more of a butterfly valve than gate valve, it has nonperiodic square wave alike pressure increase at t = 8s with a longer period of time. Zoomed image of pressure profile at point 4 shows a combination of oscillation alike in case of a system with a butterfly valve, but, the peak of the pressure is at t = 7.3s, which can be seen with the gate valve and the maximum pressure is a bit higher compared to the butterfly valve.

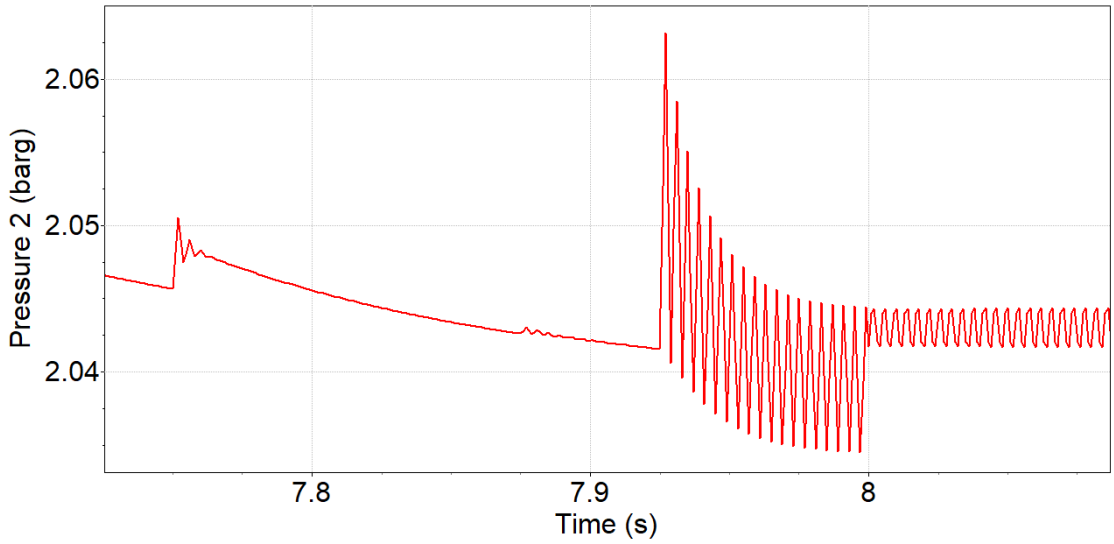

Figure 4.21. Ball valve: Pressure profile at point 4 (zoomed)

4.4. Solid concentration variation

In order to simulate the pressure profile as a function of solid concentration, it is important to determine the dependent variable, which is the steady-state-pressure, maximum pressure rise and pressure drop at point 4. It is based on the simulations, which have been carried out with different valves and the most important characteristic is the pressure profile at point 4, the other properties are somewhat the same. Table 6 & 7 show the relationship between the properties of the fluid and solid mass concentration. The pinch valve is used for all of these simulations and closing time is specified as $\Delta t = 5s$, the closure starts at t = 3s and fully closes at t = 8s. Table 12. contains the results

from simulations at different solid concentrations specifically the above mentioned determined variables. In Figure 4.22 & 4.23, the graph illustrating the relationship between solid concentrations and pressure profile can be seen.

Table 12. Pressure variables at point 4 as a function of solid concentration

Solid concentration, %	Steady state pressure,barg	Max pressure rise, barg	Max pressure drop, barg
15.0	1.93881	0.162444844	0.124685781
15.5	1.946166406	0.163060938	0.125159375
16.0	1.949845313	0.16335375	0.125406719
16.5	1.959040625	0.164130313	0.12599375
17.0	1.966398281	0.164751563	0.126463906
17.5	1.975594375	0.165525781	0.127051719
18.0	1.986631719	0.166455625	0.127759531
18.5	1.995826875	0.167229688	0.128346094
19.0	2.005024219	0.167984844	0.128949688
19.5	2.014219063	0.16875875	0.12953625
20.0	2.023415625	0.169535781	0.130124531
20.5	2.032613594	0.170310469	0.130710313
21.0	2.041808281	0.171088281	0.131297969
21.5	2.051004375	0.171841875	0.131901563
22.0	2.060199531	0.172620781	0.132485469
22.5	2.071237344	0.173548438	0.133189375
23.0	2.080432813	0.174329688	0.133773125
23.5	2.089627188	0.1750825	0.134375625
24.0	2.0988225	0.175864219	0.134960156
24.5	2.108020156	0.176639688	0.135544219
25.0	2.117215313	0.177404688	0.13614125

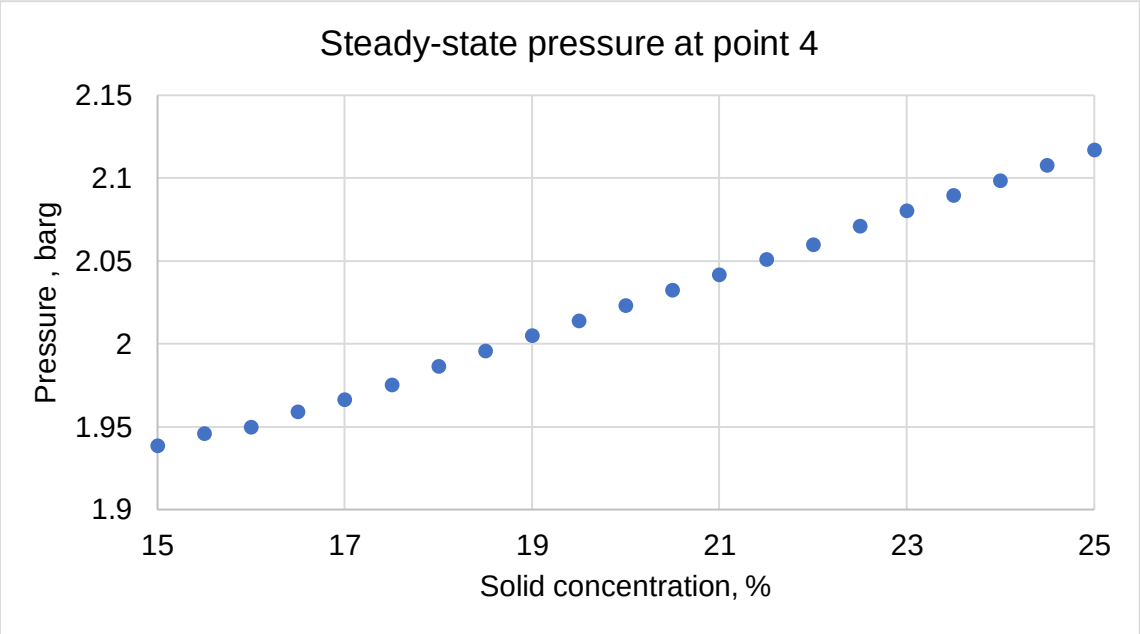

Figure 4.22. Steady-state pressure at point 4 depending on solid concentration

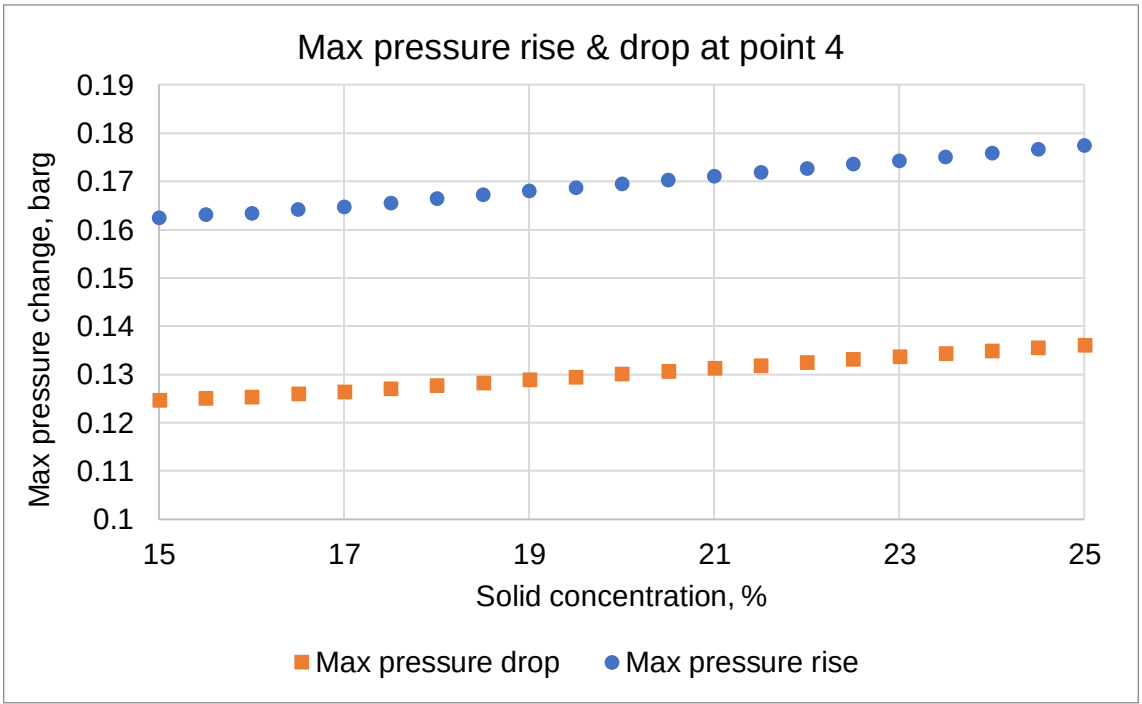

Figure 4.23. Maximum pressure changes at point 4 depending on solid concentration.

It is evident that, as solid concentration increases the steady-state pressure and maximum pressure changes increase, which is expected result since the density and the viscosity of the fluid is increasing with the solid concentration rise. Maximum pressure drop is always lower than the maximum pressure rise, which is due to damping pressure oscillation.

4.5. Valve closure time

4.5.1. Uniform valve closure

Independent variable is the valve closure time and all the other variables stay constant as solid concentration = 20%, pinch valve is used. In this case, the maximum pressure change is taken into consideration as a dependent variable due to the fact that the steady-state pressure is not dependent on the valve closure time. Valve closure time is varied from 0.05s to 10s with custom steps depending on the change.

First of all, in extreme case with valve closure time as 0.05s pressure profile can be compared with the ones with valve closure duration of 5s.

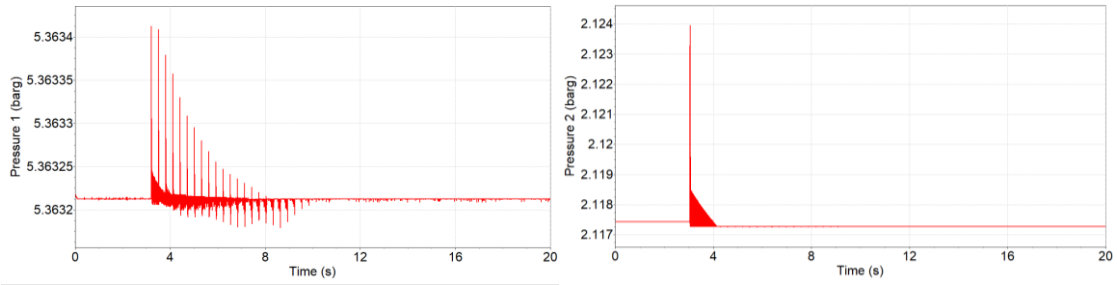

Figure 4.24. Δt = 0.05s: Pressure profile at point 1 & 2

To compare to simulations with 5s closure time, the amplitudes of the pressure oscillations at point 1 & 2 are really high, yet it is negligible in contrast to the steady-state pressure at those points.

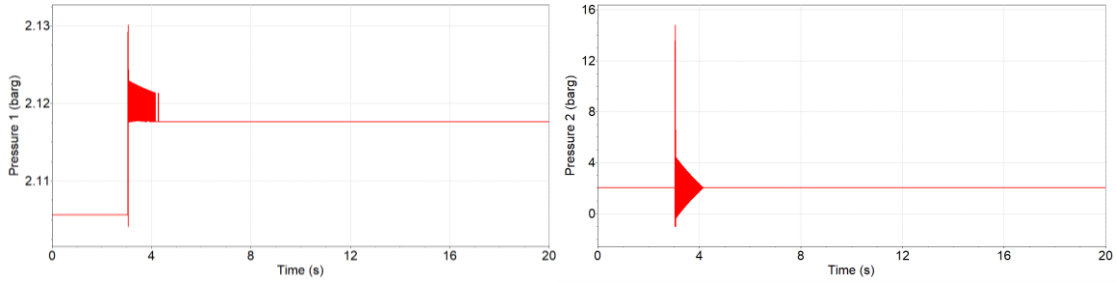

Figure 4.25. Δt = 0.05s: Pressure profile at point 3 & 4

As you can see from the figure above, the pressure at point 3 is also not increasing tremendously (increasing by 1% of the steady-state pressure). Although the pressure profile at point 4 shows an acute change in a very small amount of time, it sky-rocketed from ~2barg to ~14barg then the pressure drops below zero causing column separation. All these changes take place in a matter of 0.01 second. In this condition, it is sufficient to burst out the pipes leading to very serious damage. The pressure does not go below -1 barg, it is most likely caused by the software limitations.

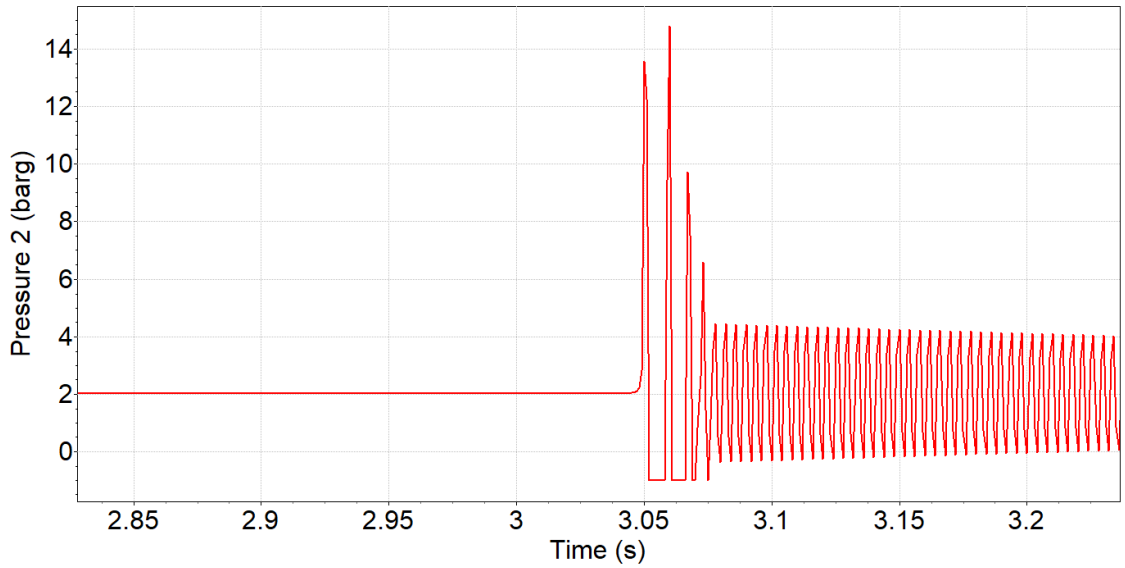

Figure 4.26. Δt = 0.05s: Pressure profile at point 4 (zoomed)

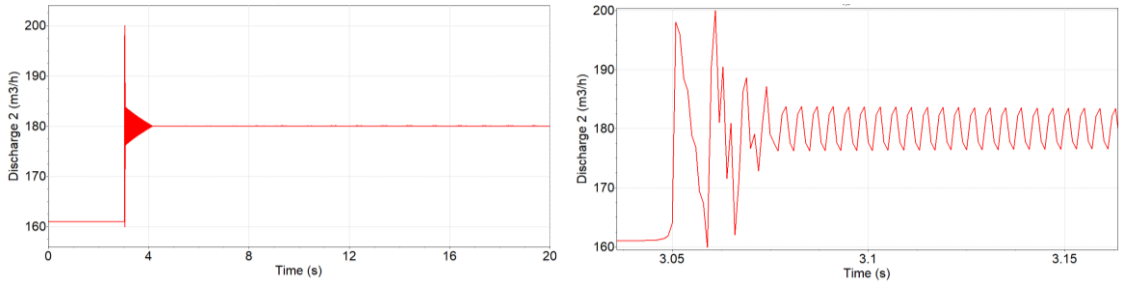

Figure 4.27. Δt = 0.05s: Discharge flow rate through point 6 (overall & zoomed)

The sudden pressure change in the pipe before the valve also affect the discharge flow rate through point 6 (point 7), due to the column separation in the pipe before the valve, the discharge flow rate through point 6 is increasing up to 200 m^3/h. It can cause failure because the pipe is not elastic enough to handle this much volumetric change in this short time period. From these results, one more dependent variable should be considered which is the maximum flow rate through point 6.

The system stabilizes in less than 3 seconds, therefore it is good to reduce the duration of the simulation to 10 seconds up to valve closure duration of 5 seconds and from there the simulation duration is increased to 15 seconds.

Maximum pressure at point 4 and the maximum flow rate through point 6 at the corresponding valve closure time is shown in Table 13 with associating graphs in Figure 4.28 & 4.29.

Table 13. Maximum pressure at point 4 and maximum flow rate through point 6

Valve closure time, s	Max pressure, barg	Max flow rate, m^3/h
0.05	14.80	199.97
0.10	12.14	199.97
0.20	8.82	190.60
0.25	7.48	188.52
0.30	6.44	186.89
0.35	5.65	185.65
0.40	5.05	184.70
0.45	4.59	183.99
0.50	4.24	183.43
0.60	3.74	182.67
0.70	3.42	182.16
1.00	2.92	181.38
1.50	2.59	180.86
2.00	2.44	180.63
3.00	2.30	180.40
6.00	2.17	180.19
9.00	2.12	180.13

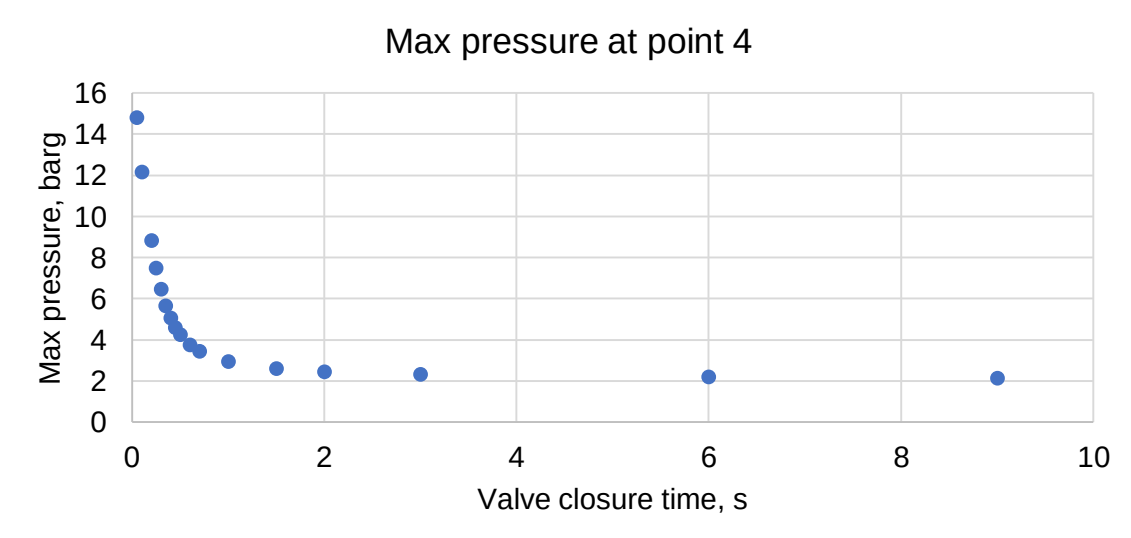

Figure 4.28. Maximum pressure at point 4 as a function of valve closure time

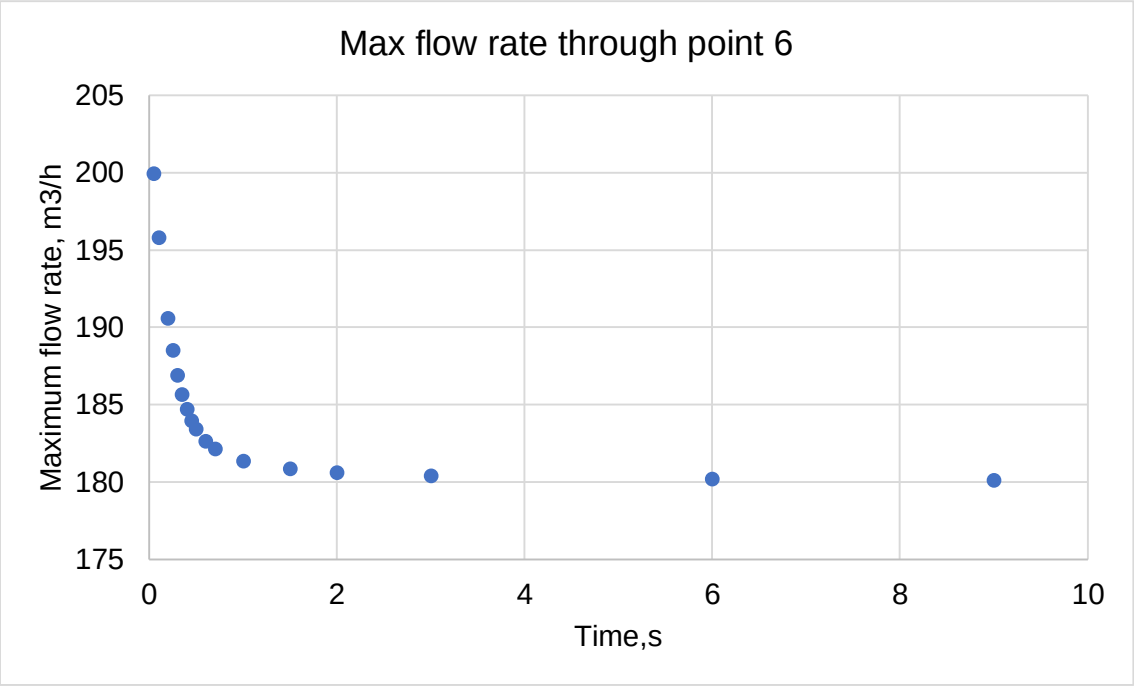

Figure 4.29. Maximum flow rate through point 6 as a function of valve closure time

From the result, it is possible to determine the optimum closure time where it is precise enough to regulate flow rate without bringing serious damage and risk. The optimum time with uniform closure would be between 1.5 seconds to 2 seconds, in this range the pressure increase is between 28% and 21% from the steady-state pressure.

4.5.2. Stepwise valve closure

The simulation can also be done with non-uniform (stepwise) valve closure time profile for the comparison between rapid closing of the valve at the beginning, gradual closing at the end and vise versa. Overall closure duration is 1 second and all the other variables will not change.

At first, the valve closes up to 20% open position in 0.1s from there it closes to 0% open position in 0.9s as shown in Figure 4.30.a), and the corresponding pressure profile at point 4 is shown in 4.30.b). Maximum pressure at point 4 is ~2.2barg, which is much lower than the original value with uniform valve closure in 1s. Maximum pressure of 2.2barg corresponds to the uniform closure of approximately 6s, thus it can be concluded as a very effective way to eliminate severe effects of water hammer.

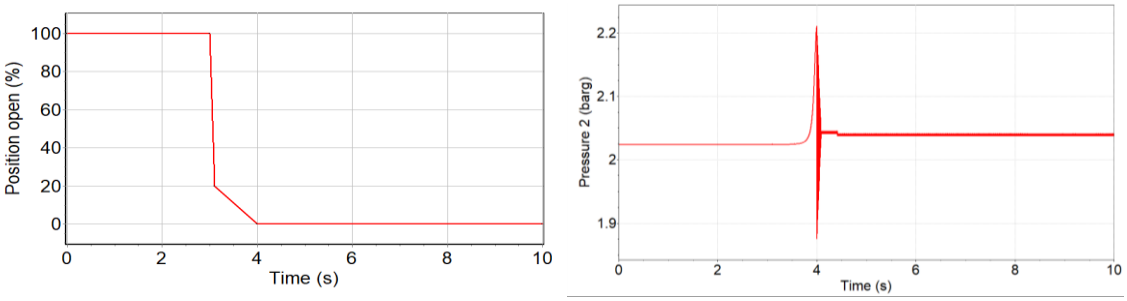

Figure 4.30. a) Valve closure time profile b) Corresponding pressure profile at point 4

As a comparison, the simulation can be carried out with reversed valve closure time profile, the valve closes slowly in the beginning and rapidly in the end as in Figure 4.31.a). From Figure 4.31.b), it is evident that pressure increase is vastly different than the last results with different valve closure time profile, the maximum pressure is ~11.3barg close to the correlated uniform closure time of ~0.17s. Thus it is not efficient to apply these type of valve closure time profile.

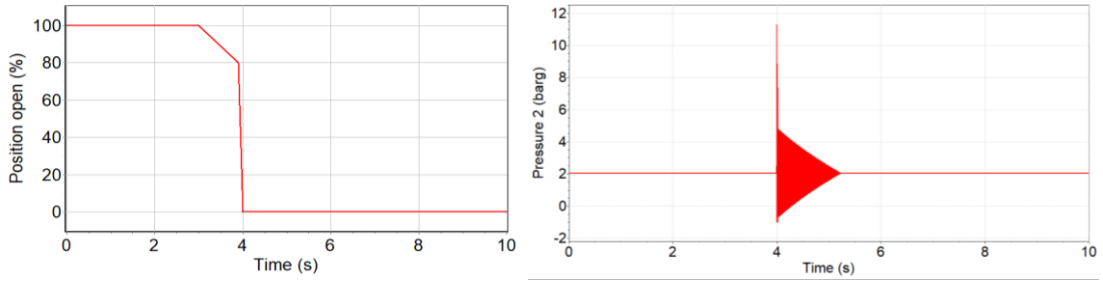

Figure 4.31. a) Valve closure time profile b) Corresponding pressure profile at point 4

4.6. Presence of a protective device

As a protective device, a surge vessel can be used (see Table 1. for clarification). The closure time is set as 1s uniformly so the difference can be seen clearly. Ideally, surge vessel should be placed before the valve (transient flow causing unit) and thus in the system, it is located as shown below.

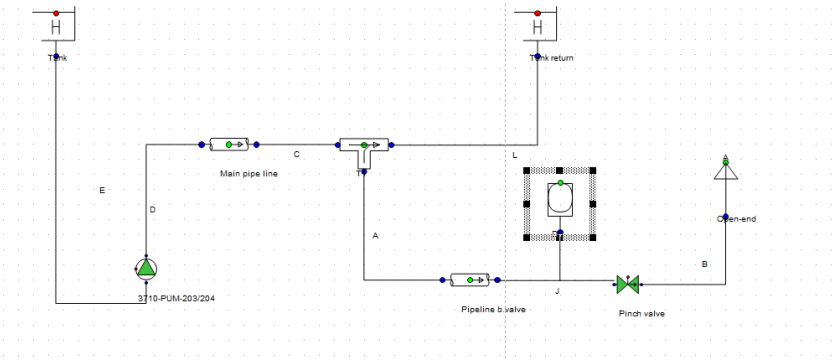

Figure 4.32. The system with a surge vessel

In order to be applicable, a surge vessel should be small and the following input is given into the simulation all values taken from a manufacturer.

Height	250.0 (mm)
Area	0.01021 (m2)
Elevation offset top	0.200000 (m)
Filling pressure	0.2000 (barg)
Laplace coefficient	1.000 (-)

Figure 4.33. Hydraulic specifications of the surge vessel [25]

The pressure profile at point 4 with the surge vessel is shown in Figure 4.34. A main role of the surge vessel is to absorb the pressure shock caused by valve closure, as a result, the pressure oscillation is much smoother and slowly damping compare to the one without surge vessel. On the other hand, the maximum pressure is at ~2.42barg, that is higher than the reduced maximum pressure of closing the valve non-uniformly (Figure 4.30.).

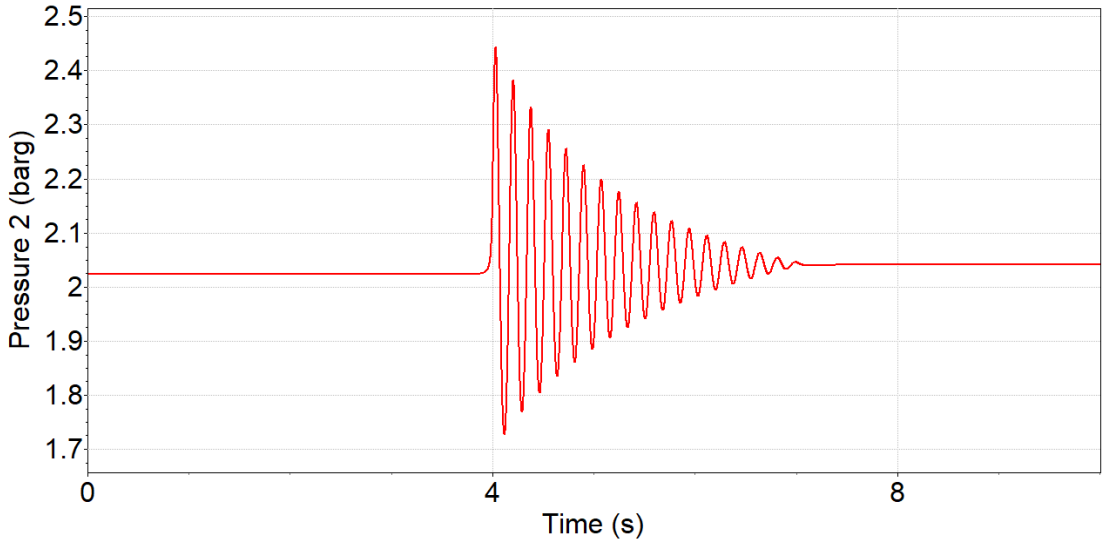

Figure 4.34. Surge vessel: Pressure profile at point 4

5. Conclusion & Recommendation

The results of the simulations show that T-junction reduces the effect of water hammer caused in the branch significantly so that in the main pipeline pressure oscillation is negligibly small. It also has proven the flow type in the main pipeline as a turbulent flow, which is very important for settling fluid such as milk of lime.

According to the results with a variety of solid concentration, the pressure profile is not considerably affected by the solid concentration in case of Newtonian fluid set-up. The settling rate of the milk of lime depends reversely on the solid concentration, therefore the recommendation would be to keep the solid concentration optimally at 20%.

Butterfly valve induces the least pressure to compare to the pinch valve, gate valve, and ball valve. With linear valve closure of 5 seconds, the pressure increase at point 4 simulated with butterfly valve is approximately 1% of the steady-state pressure at that point. On the other hand, the pinch valve generates ~10% increase in pressure at point 4. For settling slurry mixtures, the pinch valve is recommended to be used due to issues of the fluid with scaling and blockage. But it depends on the priority of the factors, if in the system the blockage can cause serious problems then the pressure increase can be reduced using another method rather than changing the valve.

Valve closure time duration and its profile have a very big influence on the pressure profile, the recommended valve closure time is 1-second using stepwise closure as in chapter 4.5.2. Theoretically, the fluid velocity profile is similar to a parabola, the fluid flows fastest in the center and slows down as it gets closer to the wall of the pipe due to friction. Thus, it also matches the results with stepwise valve closure. It may be technologically complicated to close the valve rapidly in the beginning and reduce the valve closure rate in the end, but it is possible to continuously reduce the valve closure rate to obtain a similar profile.

The result shows that the fast valve closure does not leave the fluid oscillating, it stabilizes quickly and the pressure stays constant after the valve closure. On the other hand the slower valve closure results in oscillating pressure, it means fluid in the pipe circulates which then prevents scaling.

As a protective device surge vessel was integrated into the system, the outcome was lower than expected. The surge vessel reduces the pressure effectively yet compared to stepwise closure of the valve it was not compatible.

Finally, the conclusion of the study appears to be recommending to change the profile of the valve closure rate as exponentially reducing. Protective devices can be installed for smoother and lower pressure surge.

6. Limitations of the study & future work

The study is constrained in following assumptions:

- Milk of lime is a non-settling Newtonian fluid
- Pressure loss in elbows and fitting are negligible
- No pump induced pressure surge
- No accumulated scaling in the pipeline

For the sake of simplicity, these assumptions were made based on solid evidence from other studies. The simulation software is able to calculate with slurry fluid however it requires certain properties of fluid which can only be measured with a set of precise equipment which was not available. The simulation results may be too theoretical, it would have been better if the measurement was carried out to correct the simulation model. It was reported that water hammer effect causes shift in the pipeline and in this study the shift of the pipeline was not studied.

It can be further studied combining experiment with the simulation. Scaling model can be studied and more accurate model can be developed. Other affecting variables can also be examined using simulation software. Moreover, an investigation of the relationship between pipeline shift and water effect may be interesting.

References

1. Karthrik R. Manchala. A Practical Solution to Eliminate Lime Scale Build-up in Slurry Lines; 28.08.2013.
2. Napier-Munn T, Wills BA. Wills' mineral processing technology. 2005.
3. Wylie EB, Streeter VL, Suo L. Fluid transients in systems: Prentice Hall Englewood Cliffs, NJ; 1993.
4. Parmakian J. Waterhammer analysis: Prentice-Hall New York; 1955.
5. Ferrante M, Brunone B, Meniconi S. Wavelets for the analysis of transient pressure signals for leak detection. Journal of Hydraulic Engineering. 2007;133:1274–82.
6. Chaudhry MH. Transient-flow equations. In: Applied hydraulic transients: Springer; 2014. p. 35–64.
7. Walski TM, Chase DV, Savic DA, Grayman W, Beckwith S, Koelle E. Advanced water distribution modeling and management. 2003.
8. Walski TM, Chase DV, Savic DA, Grayman W, Beckwith S, Koelle E. Advanced water distribution modeling and management. 2003.
9. Choon TW, Aik LK, Aik LE, Hin TT. Investigation of water hammer effect through pipeline system. International Journal on Advanced Science, Engineering and Information Technology. 2012;2:246–51.
10. Stanco Projects. Operation and Maintenance Manual: Lime Slaking System; 2012.
11. Boulos PF, Karney BW, Wood DJ, Lingireddy S. Hydraulic transient guidelines for protecting water distribution systems. Journal-American Water Works Association. 2005;97:111–24.
12. Controls F. Control Valve Handbook Fourth Edition [z]. Iowa, United States: Emerson Process Management. 2005.
13. Flowrox Flowsys. Inc. Heavy Duty Pinch Valves. 2018. https://www.flowrox.com/products_services/valves/pinch_valves/heavy_duty_pinch_valves.
14. Fluor Canada Ltd. Piping Isometric: 3710-RL-2056-C1B-6"-NI; 2011.
15. Fluor Canada Ltd. Piping Isometric: 3430-RL-2091-C1B-3"-NI; 2011.

16. Liu D-M. Particle packing and rheological property of highly-concentrated ceramic suspensions: φm determination and viscosity prediction. Journal of materials science. 2000;35:5503–7.

17. Krieger IM, Dougherty TJ. A mechanism for non-Newtonian flow in suspensions of rigid spheres. Transactions of the Society of Rheology. 1959;3:137–52.

18. Dabak T, Yucel O. Shear viscosity behavior of highly concentrated suspensions at low and high shear-rates. Rheologica acta. 1986;25:527–33.

19. Chong JS, Christiansen EB, Baer AD. Rheology of concentrated suspensions. Journal of applied polymer science. 1971;15:2007–21.

20. Senapati PK, Panda D, Parida A. Predicting viscosity of limestone–water slurry. Journal of minerals and materials characterization and Engineering. 2009;8:203.

21. Crane Co. Flow of fluids through valves, fittings, and pipe: Crane Co; 1988.

22. Kodura A. An analysis of the impact of valve closure time on the course of water hammer. Archives of Hydro-Engineering and Environmental Mechanics. 2016;63:35–45.

23. Projectmaterials. Butterfly Valve API 609 (Centric, Eccentric). 2017. https://blog.projectmaterials.com/valves/butterfly-valve-api-609/.

24. Young Lee. Hydraulic Ball Valve. 2018. http://www.sino-alloy.com/blog/what-is-hydraulic-ball-valve.html.

25. Hydac Technology GmbH. Hydraulic Dampers; 2012.